



UNIVERSITÀ DI PARMA

ARCHIVIO DELLA RICERCA

University of Parma Research Repository

An integrated IoT-Wi-Fi board for remote data acquisition and sharing from innovative immunosensors. Case of study: Diagnosis of celiac disease

This is the peer reviewed version of the following article:

Original

An integrated IoT-Wi-Fi board for remote data acquisition and sharing from innovative immunosensors. Case of study: Diagnosis of celiac disease / Giannetto, Marco; Bianchi, Valentina; Gentili, Silvia; Fortunati, Simone; DE MUNARI, Ilaria; Careri, Maria. - In: SENSORS AND ACTUATORS. B, CHEMICAL. - ISSN 0925-4005. - 273:(2018), pp. 1395-1403. [10.1016/j.snb.2018.07.056]

Availability:

This version is available at: 11381/2848595 since: 2021-10-08T11:14:44Z

Publisher:

Elsevier B.V.

Published

DOI:10.1016/j.snb.2018.07.056

Terms of use:

Anyone can freely access the full text of works made available as "Open Access". Works made available

Publisher copyright

note finali coverpage

(Article begins on next page)

Manuscript Number: SNB-D-18-01651R1

Title: An integrated IoT-Wi-Fi board for remote data acquisition and sharing from innovative immunosensors. Case of study: diagnosis of celiac disease

Article Type: Research Paper

Keywords: Internet of Things; Wi-Fi; smart sensor; Immunosensor; Celiac Disease; Gold Nanoparticles Screen Printed Electrodes

Corresponding Author: Dr. Marco Giannetto, PhD

Corresponding Author's Institution: Università di Parma

First Author: Marco Giannetto, PhD

Order of Authors: Marco Giannetto, PhD; Valentina Bianchi, PhD; Silvia Gentili, M.Sc.; Simone Fortunati, M.Sc.; Ilaria De Munari, PhD; Maria Careri, PhD

Abstract: A new compact diagnostic device exploiting the integration of screen printed electrode-based immunosensors and remote-controlled IoT-WiFi acquisition board has been realized and validated for diagnosis of Celiac Disease as case of study. The immunodevice is based on chemisorption of open tissue transglutaminase enzyme on the surface of gold nanoparticles-functionalized carbon screen printed electrodes. IgA and IgG anti-tissue transglutaminase target antibodies are recognized by the immobilized bioreceptor as highly specific biomarkers related to Celiac Disease. The signal from the amperometric sensor is acquired and processed through on-purpose developed IoT-WiFi integrated board, allowing for real-time data sharing on cloud services to directly notify all users (physicians, caregivers, etc.) on device outcome. The proposed solution does not require customized hardware or software. The analytical performances of the immunosensors were optimized by experimental design, obtaining diagnostically useful limit of detection (LOD) and limit of quantitation (LOQ) values (LODIgA = 3.2 AU mL⁻¹; LODIgG = 1.4 AU mL⁻¹; LOQIgA = 4.6 AU mL⁻¹; LOQIgG = 2.3 AU mL⁻¹) as well as good intermediate precision (RSD < 5%). The high discrimination capability of the IoT-Wi-Fi device between positive and negative serum control resulted to be suitable for diagnostic purposes, with outstanding statistical significance (p < 0,001)

*Research Highlights

-IoT – Wi-Fi system for rapid acquisition and sharing of data innovative immunosensors for diagnosis of Celiac Disease

-Performance suitable for @home diagnosis and point-of-care

-Versatility and suitability for wide-range clinical and diagnostic applications based on alkaline phosphatase as enzyme tag.

Comments:

Administrative Support Agent [02-Feb-11] Administrative Support Agent has DECLINED to take on this assignment.

The Editor has provided the following reason for this decision:

1. Abstract should be within (50-200 words).

R1 The abstract was reduced to exactly 200 words.

2. Please provide double line spacing in the manuscript.

R2 The whole manuscript is now double-line spaced.

3. The acknowledgement should be at the end of the paper.

R3 No acknowledgement section is required.



**UNIVERSITÀ
DI PARMA**

**DIPARTIMENTO DI SCIENZE
CHIMICHE, DELLA VITA E DELLA
SOSTENIBILITÀ AMBIENTALE**

Parma, June 11, 2018

Dear Editor,

please consider the revised version of the manuscript SNB-D-18-01651.R1 entitled "An integrated IoT-Wi-Fi board for remote data acquisition and sharing from innovative immunosensors. Case of study: diagnosis of celiac disease", by Marco Giannetto, Valentina Bianchi, Silvia Gentili, Simone Fortunati, Ilaria De Munari and Maria Careri, proposed for the publication on "Sensors and Actuators B: Chemical" as research paper. The paper is unpublished and has not been submitted for publication elsewhere.

The manuscript was thoroughly revised according to the reviewer's comments.

A point-to-point response to the comments is attached as separated file (Response to Reviewers)

In the marked version of the revised manuscript the changes are highlighted in red, while the unmarked version reports only the revised final version.

The paper deals with a very innovative study concerning the development and validation of an integrated IoT-Wi-Fi board for remote data acquisition and sharing from a disposable amperometric immunosensor aimed at diagnosis of Celiac Disease. The immunosensor is an improvement of a diagnostic devices previously developed by us (M. Giannetto, M. Mattarozzi, E. Umiltà, A. Manfredi, S. Quaglia, M. Careri, An amperometric immunosensor for diagnosis of celiac disease based on covalent immobilization of open conformation tissue transglutaminase for determination of anti-tTG antibodies in human serum, *Biosensors and Bioelectronics* 62 (2014) 325-330), now implemented on gold-nanoparticles carbon screen printed electrodes and, most importantly, integrated with the innovative data acquisition and sharing system. The new system was validated for the determination of anti-tissue transglutaminase IgA and IgG in diluted human serum, showing excellent analytical performance, suitable for diagnostic purposes. The capability of the IoT-Wi-Fi device in terms of discrimination between positive and negative serum control resulted to be remarkable. The device is not intended for quantitative assay, but is conceived as a compact, portable, user-friendly front-line screening tool usable for out-of-hospital self-diagnosis, with the additional gain of the possibility to carry out the data sharing and managing. A fundamental feature of the developed system consists in its high versatility and transversality, being the remote-controlled board suitable for all the sensing devices conceived for diagnostic purpose and based on the use of alkaline phosphatase as labelling enzyme.

Best regards,

Prof. Marco Giannetto, PhD

Associate Professor

Dipartimento di Scienze Chimiche, della Vita e della Sostenibilità Ambientale

Università di Parma

Parco Area delle Scienze 17/A

43124 Parma

e-mail: marco.giannetto@unipr.it

UNIVERSITÀ DI PARMA

Parco Area delle Scienze, 11/A - 43124 Parma

www.unipr.it

Dear Editor,

The manuscript was thoroughly revised according to the reviewer's comments.

A point-to-point response to the comments is reported as follows: (responses to the comments are highlighted in red)

Reviewer #1:

The manuscript "An integrated IoT-Wi-Fi board for remote data acquisition and sharing from innovative immunosensors. Case of study: diagnosis of celiac disease ", authored by Valentina Bianchi et. al., is an interesting work reporting -IoT-Wi-Fi system for rapid acquisition and sharing of data innovative immunosensors for diagnosis of celiac disease. They claim that the obtained immunosensors show good performance for sensing of anti-tTG human IgA and IgG. The results demonstrated here is interesting and the quality of the presentation is suitable. However, there are some revisions should be addressed carefully before the final acceptance.

1. In section of introduction, the research dynamics in this field need to be reviewed, especially the work that is similar to this paper needs citations and comments. In addition, there are too few references.

R1.1: We would like to thank the reviewer for the suggestion; accordingly, the introduction was improved with a more thorough overview of the state-of-the-art on wireless chemical sensors and biosensors evidencing the specific advantages of the device developed by us, with respect to other reported in literature. As requested by the reviewer, new references were included in the text.

2. Please add interference study of the obtained immunosensor.

R1.2: We would like to thank the reviewer for the valuable and constructive suggestion. We carried out new experiments aimed at assessing in more detail the specificity of the developed immunosensor. The findings of such experiments were included in a new paragraph (3.3), entitled "Interference study". We chose anti-deamidated gliadin antibodies as biomarkers potentially occurring in serum samples from subjects affected by Celiac Disease. As reported in the new paragraph, no significant difference was observed both in presence and in absence of different concentrations of anti-deamidated gliadin antibodies both for positive (anti-tTG IgA and IgG) and negative serum controls. The interference was not extended also to anti-endomysium antibodies, since they are no longer considered specific and reliable biomarkers for diagnosis of Celiac Disease, as reported in several clinical studies (see: **Arie Levine et al**, Comparison of Assays for Anti-endomysial and Anti-transglutaminase Antibodies for Diagnosis of Pediatric Celiac Disease, *Gastroenterology*, Vol 2, February 2000, p. 122-125).

According to the results of the interference study, we were able to confirm the specificity of the sensor, already assessed by validation in properly diluted human serum.

Reviewer #2:

The manuscript proposed a remote-controlled IoT-WiFi immunodevice for diagnosis of Celiac Disease. The concept is proofed by using a screen printed electrode-based immunosensors combined with an IoT-WiFi integrated board for amperometric signal readout. The immunosensor was constructed by chemisorption of open tissue transglutaminase enzyme on the surface of gold nanoparticles functionalized carbon screen printed electrodes. The signal was readout by

attaching IgA and IgG anti-tissue transglutaminase target antibodies on the electrode surface through immunoreactions. The analytical method was not new. The integration of immunosensors with IoT-WiFi to realize remote real-time data sharing on cloud services was an ideal concept. However, the electrochemical techniques such as DPV was doubted to be able to conduct by IoT-WiFi. Also, the reported data were mainly performed by LMP91000. All data reported in 3.3 should be supported by the measurements performed with LMP91000 at the same conditions.

R2

We thank the reviewer for the comments; regarding the real-time data sharing on cloud, the authors would like to clarify what they meant: the real-time has not to be intended as a continuous streaming of raw data from the sensor to the cloud but as an immediate sharing of the data elaboration result (positive/negative serum control) with all the interested people (physicians, caregivers, users themselves, etc..). Data from the sensor are acquired on a time interval and then processed to get a positive or negative result. Data elaboration can be carried out both on board, limiting data transmission and therefore battery consumption, or on cloud without any change in the result. We chose the latter for prototypal purposes.

Furthermore, in the prototypal version, the communication with a cloud service was proved, demonstrating the soundness of our approach.

The data reported in section 3.4 (3.3 in the unrevised version of the manuscript) were in fact acquired with LMP91000 (integrated in our IoT-WiFi device), as shown in Figures 11, 12, 13 and 14. Figures 2 and 4, as well as the caption of Figure 4 were modified in order to identify more clearly the architecture of the device and the integration of our IoT-WiFi device in a standard Wi-Fi network.

As for the data reported in section 3.2 (quantitative calibration lines), we reaffirm that the device developed in this work is not intended for quantitative assay but is designed as a screening tool usable for out-of-hospital self-diagnosis, aimed at efficiently discriminating among anti-tTG IgA/IgG positive and negative serum samples, as already stated in section 4 of the unrevised manuscript.

.

An integrated IoT-Wi-Fi board for remote data acquisition and sharing from innovative immunosensors. Case of study: diagnosis of celiac disease

Marco Giannetto^{a}, Valentina Bianchi^{b*}, Silvia Gentili^a, Simone Fortunati^a, Ilaria De Munari^b, Maria Careri^a*

^a Dipartimento di Scienze Chimiche, della Vita e della Sostenibilità Ambientale, Università di Parma. Parco Area delle Scienze 17/A, 43124 Parma (Italy)

^b Dipartimento di Ingegneria e Architettura, Università di Parma. Parco Area delle Scienze 181/A, 43124 Parma (Italy)

**Corresponding Authors:*

Marco Giannetto (marco.giannetto@unipr.it); Valentina Bianchi (valentina.bianchi@unipr.it)

Abstract

A new compact diagnostic device exploiting the integration of screen printed electrode-based immunosensors and remote-controlled IoT-WiFi acquisition board has been realized and validated for diagnosis of Celiac Disease as case of study. The immunodevice is based on chemisorption of open tissue transglutaminase enzyme on the surface of gold nanoparticles-functionalized carbon screen printed electrodes. IgA and IgG anti-tissue transglutaminase target antibodies are recognized by the immobilized bioreceptor as highly specific biomarkers related to Celiac Disease. The signal from the amperometric sensor is acquired and processed through on-purpose developed IoT-WiFi integrated board, allowing for real-time data sharing on cloud services to directly notify all users (physicians, caregivers, etc.) on device outcome. The proposed solution does not require customized hardware or software.

The analytical performances of the immunosensors were optimized by experimental design, obtaining diagnostically useful limit of detection (LOD) and limit of quantitation (LOQ)

values ($\text{LOD}_{\text{IgA}} = 3.2 \text{ AU mL}^{-1}$; $\text{LOD}_{\text{IgG}} = 1.4 \text{ AU mL}^{-1}$; $\text{LOQ}_{\text{IgA}} = 4.6 \text{ AU mL}^{-1}$; $\text{LOQ}_{\text{IgG}} = 2.3 \text{ AU mL}^{-1}$) as well as good intermediate precision ($\text{RSD} < 5\%$).

The high discrimination capability of the IoT-Wi-Fi device between positive and negative serum control resulted to be suitable for diagnostic purposes, with outstanding statistical significance ($p < 0,001$)

1. Introduction

Wi-Fi infrastructures are nowadays highly diffused in the home context thanks to the comfort (or the need) to have a wireless gate to Internet. This wireless technology appears to be the most suitable for developing portable and connected devices usable autonomously by the user at home. In fact, Wi-Fi data transmission allows to take advantage of the infrastructure already present in the home environment or can be based on off-the-shelf solutions (e.g. standard modem/router) to ensure the connectivity to a diagnostic device, for example. This vision perfectly fits with the paradigm of the Internet of Things (IoT) [1]: in such a context, a sensor becomes an IoT node capable to acquire and send data independently but, at the same time, cooperating with other sensing devices, thus exploiting a maximally open network. Using this infrastructure, the data can be straightforwardly sent to a cloud platform and here processed [2].

Currently, wireless chemical sensors and biosensors are attracting a great deal of interest [3]. In fact, wireless technology simplifies the system architecture and improves the ease-of-operation of the device with respect to wired solutions [4]. Combining advances in wireless technology and chemical sensing has led to the development of devices with application in different fields [5-7]: among these, health care is of particular importance [8]. In addition, the application of the IoT vision to wireless chemical sensors designed for this application further increases the relevance of such devices. Since Nowadays cloud services allow to send messages (e.g. text messages, tweets, etc.), this feature can be exploited to send the diagnostic data directly on the phone/pc of the user/physician, without the necessity of developing custom apps, which represent an advantage with

respect to other solutions presented in literature [9,10]. Some of them are based on smartphones with dedicated adaptors [11-13]. For instance, Xu et al. [12] and Steinberg et al. [13] presented a RFID/NFC solution. Because of the peculiarities of the communication protocols involved, this solution requires the availability of a smartphone or a gateway at a very short distance [14,15]: the smartphone becomes actually a part of the data acquisition system, thus reducing the advantage in terms of cost and size of the overall system. Very recently, a wireless potentiostat, based on a novel low-complexity wireless unit exploiting a short-range inductive telemetry was presented [16]. Also in this case, an Internet gateway would be mandatory in real world use, thus complicating the system architecture. A point-of-use platform for multivariate analyses based on the use of a potentiostat exploiting Bluetooth connectivity was reported: complex and multivariate data can be locally processed with a dedicated app or can be forwarded to a cloud service exploiting the smartphone connection [17]. Compared to these solutions, the integration of Wi-Fi and the IoT paradigm allows to exploit a unique hardware platform and a direct connection to the Internet without the need of a gateway, reducing the complexity of the system architecture, and therefore the costs associated with it, and improving ease-of-use.

Wi-Fi protocol has a well-known disadvantage with respect to other wireless standard, such as Bluetooth Low Energy (BLE) or ZigBee, regarding a higher power consumption: this could be overcome by some low-power design strategies. It has been proved that by adjusting the radio activity period it is possible to obtain excellent performances in terms of battery life for devices developed to transmit data with high frequency (e.g. environmental or personal data logger) [18]. In the case of chemical sensing devices, the frequency of data transmission is certainly much lower, so this problem is mitigated.

It is worth noting that these miniaturized portable devices will not have the same processing capabilities and measurement resolution of traditional benchtop instruments: however, the purpose of these devices is to provide an indication of occurrence of a particular disease-related biomarker and in some cases to address the user to further medical examination rather than to carry out an

accurate measurement. In this context, the target of the assay is the discrimination between positive (sick) and negative (healthy) samples.

Data gathered from diagnostic sensors can be locally processed and then transmitted over the Internet: this allows for a remote control of the user's health status. The idea behind is that of *online* monitoring: the adoption of technological solutions allows for follow-up of patients in their own homes without the need for constant interaction with a physician, and, in some cases, for building a database of parameters related to a particular pathology that can be useful for analyzing related statistics.

Electrochemical immunosensors represent a powerful tool for domiciliary self-diagnosis, as they require low-cost and simplified instrumentation that can be miniaturized in order to develop portable devices.

The peculiarities of immunosensors rely in shorter analysis time and in the possibility to perform quantitative or semi-quantitative analyses not limited to simple qualitative screening usually associated to conventional immunochemical approaches such as Enzyme Linked Immunosorbent Assay (ELISA) methods. Currently an increasing interest is focused on the application of these devices to diagnosis and monitoring of autoimmune diseases [19]. Among these, Celiac Disease (CD), showed in the last decades a more and more frequent occurrence. For this reason, the discovery of new reliable biomarkers had as a consequence the development of high-performance immunosensors devoted to detection/quantification of specific CD-related biomarkers.

CD occurs in genetically predisposed individuals as a result of ingestion of gluten, the protein component of cereals such as wheat, rye, etc. CD is characterized by an immune response triggered by the recognition of gliadin peptides, the alcohol-soluble component of gluten, along with an increase of T-lymphocytes in the intestinal mucosa. This results in inflammatory processes and spoilage of the latter, examined via duodenal biopsy, together with the expression of specific antibodies proved to be disease-related biomarkers. Among these, the anti-tissue transglutaminase antibodies (anti-tTG) directed versus the open conformation of transglutaminase enzyme can be

determined and monitored via hematic assays, both in the IgG (gamma-immunoglobulines) and IgA (alpha-immunoglobulines) forms to avoid false negative responses associated with IgA deficiency.

In this scenario, an amperometric immunosensor based on covalent immobilization of the enzymatic receptor (Open tTG[®]) in its open conformation for the determination of antibodies anti-tTG has been recently developed by our research group [20].

In such a context, the aim of the present study was to realize and validate a compact diagnostic device and to optimize the previously cited amperometric immunosensor in order to fit the new IoT-Wi-Fi based diagnostic tool. The immunodevice is based on the direct chemisorption of Open tTG[®] on the surface of Gold NanoParticles-functionalized Carbon Screen Printed Electrodes (GNP-CSPEs). Anti-tTG target antibodies are recognized from the immobilized bioreceptor and subsequently detected through alkaline phosphatase-labelled anti-human IgA/IgG.

The so modified GNP-CSPEs are then connected to the newly developed IoT-Wi-Fi board for remote data acquisition. The measurements are then processed and transmitted through a standard Wi-Fi connection and stored in an open cloud platform. Details about the hardware and the software solutions are given in the experimental section.

2. Experimental

2.1. Materials

Trizma[®] base, ethylenediaminetetraacetic acid disodium salt dihydrate (Na₂EDTA), DL-dithiothreitol (DTT), sodium chloride (NaCl), calcium dichloride hexahydrate (CaCl₂·6H₂O), albumin from bovine serum (BSA), magnesium chloride anhydrous (MgCl₂), Tween[®] 20 and human serum were purchased from Sigma-Aldrich (Milan, Italy). Hydroquinone diphosphate (HQDP) was from Metrohm Italiana (DropSens DRP-HQDP) (Origgio, Italy).

Double-distilled and deionized water purified with a Milli-Q system was used for the preparation of the buffered solutions.

“Enzyme buffer” (EB) was prepared according to the following composition: 0.02 M Trizma® base, 0.001 M Na₂EDTA, 0.001 M DTT, 0.15 M NaCl, 0.01 M CaCl₂·6H₂O (pH 7.2). Tris buffered saline (TBS) was prepared according to the following composition: 0.1 M Trizma® base, 0.02 M MgCl₂ (pH 7.4). “Sample buffer” (SB) and “wash buffer” (10×) were contained in ELISA kits. Diluted “wash buffer” (WB 1×) was prepared by dilution of “wash buffer” 10× in water. “Reading buffer” (RB) was prepared according to the following composition: 0.1 M Trizma® base, 0.02 M MgCl₂ (pH 9.8).

Human tissue transglutaminase stabilized in its open conformation (Open tTG[®]) was supplied from Zedira (Darmstadt, Germany). In order to maintain the open conformation, working solutions of open-tTG were prepared in EB. ZediXclusive Open tTG[®]-Ab (IgA) and ZediXclusive Open tTG[®]-Ab (IgG) ELISA kits were purchased from Zedira. Each kit contained six calibrator solutions of anti-tTG antibodies (0, 1, 3, 10, 30, 100 AU mL⁻¹) and a positive and a negative control. For the assessment of unknown samples, the kits’ instructions established normal (negative) range (< 2.6 AU mL⁻¹), threshold value (3.0 AU mL⁻¹), equivocal range (2.6-3.5 AU mL⁻¹) and positive range (> 3.5 AU mL⁻¹). Alkaline phosphatase-labelled rabbit anti-human immunoglobulins IgA (anti-H-IgA-AP) and IgG (anti-H-IgG-AP) were from Sigma-Aldrich. Open tTG[®], anti-H-IgA-AP and anti-H-IgG-AP were aliquoted and stored at -20 °C after delivery.

Interference studies were performed by using ZediXclusive DGPx1-ab (IgA) and ZediXclusive DGPx1-ab (IgG) ELISA kits were purchased from Zedira GmbH (Darmstadt, Germany).

2.2. Instrumentation

Immunosensors were assembled on GNP-CSPEs purchased by Metrohm Italiana (DropSens DRP-110GNP) (Origgio, Italy).

All electrochemical measurements were performed with a μ Autolab III electrochemical workstation (EcoChemie, Utrecht, NL) equipped with GPES 4.9 version customized software and connected to DropSens DRP-DSC plug.

2.3. Immunosensor set-up

In order to perform the enzyme covalent linking, the GNP electrodes were incubated for 3 h at room temperature with 25 μ L of open-tTG solution, properly diluted (see section 3.1) in EB from the original stock solution. After removal of unreacted enzyme by accurate washing with EB, a blocking treatment, aimed at preventing unspecific responses during sample incubation, was carried out by casting 50 μ L of a 20 mg mL⁻¹ solution of BSA dissolved in EB on each electrode for an incubation time of 60 min, followed by washing with the same buffer. The ready to use GNP/Open-tTG modified electrodes were dried and stored at 4 °C when not in use.

Detection of anti-tTG antibodies was carried out by incubating the immunosensors with 20 μ L of sample (standard solutions from ELISA kits or 1:100 diluted human serum) for 60 min. The sensors were then carefully washed with WB and finally with TBS in order to prevent unspecific binding phenomena. Subsequently, each immunosensor was incubated for 60 min with 50 μ L of anti-H-IgA-AP or anti-H-IgG-AP, diluted in SB as described in section 3.1, in order to reveal anti-tTG antibodies previously immobilized on the electrodic surface. The protocol implemented for the realization of the immunosensors is schematically represented in Scheme 1: after direct chemisorption of the tTG enzyme on the electrodic surface, a blocking with BSA was carried out. Under these conditions the sensor is ready to be stocked until use, consisting in incubation of the sensing surface with the 1:100-diluted serum sample, followed by incubation with AP-conjugated

anti-H-IgA or -IgG and amperometric reading of the assay. The reading of the electrochemical immunoassay was performed by Differential Pulse voltammetry (DPV) measurements using 50 μL of a 1 mg mL^{-1} solution of HQDP dissolved in RB. DPV curves were acquired by scanning the potential between -0.5 V and +0.3 V (step potential= +0.00495 V, modulation amplitude= +0.04995 V, modulation time= 0.102 s, interval time= 0.4 s) and recording the signal ascribable to the oxidation of hydroquinone HQ, generated by AP-promoted enzymatic dephosphorylation of HQDP, to Quinone (Q). The peak current is associated with the amount of produced HQ, which is related to the concentration of the immobilized anti-H-IgA (or IgG)-AP. The amount of immunosorbed anti-H-IgA (or IgG)-AP is finally related to the concentration of the anti-tTG target antibodies in the incubated sample. At least three replicate measurements were carried out for all standards and samples. Intermediate precision was obtained performing three replicated measurements for each concentration levels on independently fabricated immunosensors.

Method validation was performed by calculating limit of detection (LOD) and limit of quantification (LOQ) according to “Eurachem Guidelines” [21].

2.4. Experimental design

The experimental response was optimized in terms of P/N ratio (P=positive control; N=negative control) in order to assess the best concentrations of *i*) the Open tTG[®] solution used for the immobilization of the enzymatic receptor and *ii*) of the reading anti-H-IgA(or IgG)-AP antibodies. Previously, ANOVA tests were carried out with the aim of assessing the significance of factors subjected to optimization by means of a 3² three-levels Full Factorial Design (FFD) [22]. Each of the nine experiments was replicated three times and acquired under randomized sequence. All statistical calculations were performed using the Statgraphics software package (Statgraphics Technologies Inc., Virginia, USA).

2.5. IoT Wi-Fi Acquisition Device

The acquisition system consists of two parts: an analog front-end (AFE) and a data acquisition and processing unit. The AFE is based on the integrated potentiostat LMP91000, for the cell conditioning and current detection resulting from the enzyme reaction occurring on GNP-CSPEs. The AFE is connected to a Wi-Fi based System on Chip (CC3200) for data sampling, processing and transmission. For preliminary tests, a prototypal sensor based on LMP91000 and CC3200 development boards was designed. The whole system is shown in Figure 1.

The prototype dimensions ($18 \times 5.7 \times 2.7$ cm), although conditioned by those of the development boards, are definitely reduced compared to a traditional acquisition system. Further reduced size is expected in the engineered version.

In the following subsections both AFE and Microcontroller Unit (MCU) are described and detailed.

2.5.1. Analog Front End

To read the electrochemical signal from the cell implemented on GNP-CSPEs, a potentiostat performing DPV scans was exploited: for this purpose the LMP91000 [23], an integrated potentiostat by Texas Instruments, was used (Figure 2).

This circuit can be programmed through an I2C interface to generate an appropriate bias voltage (V_{bias}), applied between the control (V_{ce}) and reference (V_{re}) electrodes, capable of conditioning the cell. V_{bias} , in the present case of study related to the novel immunosensor for anti-tTG antibodies determination, should range from -0.6V to 0.5V. The LMP91000 allows to select up to 27 discrete voltage levels for the bias signal. These levels are defined as a percentage of a voltage reference V_{ref} : the LMP91000 allows the selection between an internal reference (3.3V) or a custom external one. The internal reference was selected allowing to achieve the desired span without adding other components. In order to have negative values for V_{bias} , V_{ref} should have a strictly positive value. In

LMP91000 V_{ce} , can be programmed as 20%, 50% or 67% in respect to V_{ref} . It is worth to note also that, since the potentiostat has a single supply voltage circuitry, V_{ce} , V_{re} , V_{we} and V_{out} must be equal or major than zero: this imply that the following relationship should be verified

$$V_{ce} \geq V_{bias}$$

With the given voltage range, all values that is possible to program in the LMP91000 are compatible with the equation above. A value of 0.66V corresponding at 20% of V_{ref} was selected: this permits to maintain the voltages in a range directly compatible with the inputs of the MCU module, as described below, removing the need of a dedicated interface circuitry.

Once defined V_{ref} and V_{ce} , a bias signal was generated using the maximum possible number of levels to achieve the maximum resolution in reading the cell. In particular, starting from a -24% of the V_{ref} , 34 levels were considered, according to the Figure 3, to obtain exactly the desired range.

2.5.2. IoT Wi-Fi Module

The system-on-chip CC3200 by Texas Instruments was chosen for the device core. This SoC integrates an MCU with an ARM Cortex-M4 architecture and a network processor compliant with the IEEE 802.11b/g/n network protocol radio. This makes the whole system Wi-Fi certified.

The CC3200 is mounted on a development board (LaunchPadXL board [24]) that was used as a motherboard to develop the first version of the acquisition system. The working and reference electrodes and V_{out} pins from the LMP91000 board are connected to Analog to Digital inputs of the CC3200. Since the ADC inputs can manage voltages below 1.4V, and all the resulting voltage are in this range, there is no need of an interface between the two boards.

In the present study a cloud-based framework was adopted in order to allow for remote monitoring. The system “intelligence” can be distributed among the sensing device themselves (“smart” object), and external, cloud-based services. For prototypal purposes, data elaboration was performed directly on the cloud platform, but the same operations can be carried out also directly on the MCU,

without any change in the result but lowering the battery consumption of the whole device thanks to the limitation of the energy hungry Wi-Fi transmission phases. In Figure 4, a generic architecture is shown. The data flowing from the end device go straightforwardly through the modem/router via Wi-Fi Protected Access (WPA) standard protocol to be stored and processed in the Internet cloud. The wide coverage of Wi-Fi router makes easier to ensure stable sensor connection over a large area. Once delivered to the cloud, sensor data are stored and subsequently processed, in order to extract meaningful information. The sensor can be connected straightforwardly to different cloud environment by suitably coding the access method into the device firmware. The cloud environment also hosts a full set of analytical functions and converting raw sensor data into accessible information. Both raw data and synthesized analytics outcomes are then accessible through the cloud methods. In the present work an IoT open platform Thinkspeak©, which is a cloud platform supporting MATLAB data analytics, was adopted. The choice of this platform is not binding, but any other cloud platform (e.g. IBM Bluemix, Microsoft Azure etc), can be exploited as well. In Thinkspeak, using Representational State Transfer (REST) Application Programming Interface (API), it is possible to create and modify channels in which store the data for the subsequent elaboration. Details about the signal processing and elaboration are given in section 2.6.

2.6. Signal processing

The measured voltages are then processed to extrapolate the cell current due to the chemical reaction.

A current value is calculated for each point of the bias signal following the equation

$$I = \frac{V_{out} - V_w}{G}$$

where V_{out} is the LMP91000 output voltage (Figure 2), V_w is the reference voltage and G is the programmable TransImpedance Amplifier (TIA) gain. For the TIA gain a value of 7000 was

selected to avoid signal saturation. To detect a positive diagnosed user or to a negative one, the value of the peak of the current computed as the difference between the current on the bias signal (V_{bias}) rising edge and that on the falling edge has to be evaluated. This leads to 17 measurement points for each acquisition. It has to be noticed that the number of acquisition points is considerably lower to that obtainable from bench-top instruments: as already mentioned, however, this resolution is perfectly compatible with the discrimination of the disease-positive users and the negative ones, as will be demonstrated subsequently. In Figure 5 an example of measured bias signal and currents is given.

As the baseline of the differential current (baseline drift) is frequently not perfectly parallel to the x-axis, it is not possible to apply simple methods for searching the maximum to evaluate the amplitude of the peak in the obtained current waveform. For this purpose, before peak evaluation, a baseline search and calculation algorithm was introduced for each measurement. Four absolute minimum points were identified for each waveform and a baseline was estimated using a linear polynomial fitting. This baseline is then used as a reference to calculate the actual peak amplitude, as shown in Figure 6.

3. Results and discussion

3.1. Optimization of the response

In order to find the optimal concentration values of Open tTG[®] (factor 1) and anti-H-IgA-AP or anti-H-IgG-AP (factor 2), a 3^2 three-levels FFD was performed. Two independent experimental datasets were acquired for anti-tTG IgA and IgG, considering as response variable the P/N ratio, calculated from the peak current values related to positive (P) and negative (N) control samples. For detection of anti-tTG IgA antibodies the explored concentration levels of the Open tTG[®] were $4.58 \mu\text{g mL}^{-1}$, $9.16 \mu\text{g mL}^{-1}$, $18.32 \mu\text{g mL}^{-1}$, whereas in the case of anti-tTG IgG the concentration set for Open tTG[®] was $9.16 \mu\text{g mL}^{-1}$, $18.32 \mu\text{g mL}^{-1}$, $45.8 \mu\text{g mL}^{-1}$. As for the second optimized factor

(anti-H-IgA(or IgG)-AP antibodies) the explored concentration levels for anti-H-IgA-AP were 0.5 $\mu\text{g mL}^{-1}$, 1 $\mu\text{g mL}^{-1}$, 2 $\mu\text{g mL}^{-1}$, whereas for anti-H-IgG-AP concentrations ranged from 1 $\mu\text{g mL}^{-1}$ to 4 $\mu\text{g mL}^{-1}$.

The significance of the main effects and of their reciprocal interaction was checked by 2-way ANOVA with Bonferroni post hoc test. In the case of the determination of target anti-tTG IgA antibodies, both factors and their interaction resulted to be significant ($p < 0.001$). As for IgG antibodies, the Open tTG[®] concentration effect was significant with $p < 0.005$, whereas anti-H-IgG-AP antibodies and binary interaction effects were significant with $p < 0.001$.

The Open tTG[®] and anti-H-IgA-AP concentrations leading to an optimal P/N ratio for the determination of IgA anti-tTG antibodies were, respectively, 4.58 $\mu\text{g mL}^{-1}$ and 1 $\mu\text{g mL}^{-1}$, as deduced from the ANOVA interaction plot shown in Figure 7. Analogous experiments carried out for the determination of IgG anti-tTG antibodies gave concentrations of 9.16 $\mu\text{g mL}^{-1}$ and 1 $\mu\text{g mL}^{-1}$ as optimal respective values for Open tTG[®] and anti-H-IgG-AP, as from ANOVA interaction plot shown in Figure 8. Under these conditions the immunosensor was capable to quantify both IgA and IgG antibodies in a diagnostically useful concentration range.

3.2. Analytical performance

The immunosensor performance was evaluated for anti-tTG human IgA and IgG by incubation of the calibrating solutions included in the ELISA kits. Linearity of the response was checked over the 0-100 AU mL⁻¹ concentration range and assessed over the 0-30 AU mL⁻¹ range. As can be observed from the calibration functions reported in Figures 9 and 10, the best sensitivity was achieved in the case of anti-tTG human IgG. Accordingly, LOD values analytically useful for diagnostic purposes were 3.2 AU mL⁻¹ for IgA and 1.4 AU mL⁻¹ for IgG. LOQ values of 4.6 AU mL⁻¹ and 2.3 AU mL⁻¹ were calculated, respectively.

Concerning the intermediate precision of the measurements obtained using the sensors, good results were achieved, giving Relative Standard Deviation (%RSD) values <5% for both IgA and IgG anti-tTG.

3.3. Interference study

The specificity of the immunosensing device was assessed by interference studies carried out using anti-deamidated gliadin (DGPx1-Ab) human IgG and IgA antibodies, chosen as biomarkers potentially occurring in serum samples from subjects affected by Celiac Disease. In fact, although anti-tTG antibodies are currently considered as the most specific serological biomarkers associated to CD, anti-deamidated gliadin antibodies are frequently expressed, especially in pre-diagnostic stage, when the subject has not yet undertaken the gluten-free diet. For this purpose, we evaluated the response of the immunosensor to DGPx1-Ab both in presence and absence of anti-tTG. Negative serum controls spiked with DGPx1-Ab IgA and IgG at different concentrations (3, 18 and 100 U/mL; threshold value < 6.7 U/mL) showed in all cases current responses not significantly different ($p>0,05$) from non-spiked negative serum controls. Furthermore, anti-tTG-positive serum control spiked with DGPx1-Ab of both isotypes gave responses not significantly different ($p>0,05$) from the non-spiked positive serum controls, keeping the P/N ratio reported in section 3.1.

3.4. Acquisitions with the Iot-WiFi device

On the basis of the optimized experimental conditions assessed with the conventional instrumentation (potentiostat), additional datasets were acquired with the innovative IoT-WiFi device developed within this study, in order to test its performance. For this purpose, we acquired signals from 1:100 diluted positive and negative human serum controls. Selections of signals

recorded for anti-tTG IgA and IgG are reported in Figures 11 and 12, respectively (4 replicated acquisition for both positive and negative IgA and IgG serum controls).

The significance of the difference between positive and negative human serum controls was verified by 1-way ANOVA with Bonferroni post-hoc test, for the determination of both anti-tTG antibodies IgA and IgG. The negative and positive datasets resulted to be different with a very high significance level ($p < 0.001$)

The box-and-whiskers plots for IgA and IgG are reported in Figures 13 and 14.

4. Conclusions

The capability of the IoT-Wi-Fi device in terms of discrimination between positive and negative serum control resulted to be remarkable and suitable for diagnostic purpose, also considering the specificity with respect to other potentially occurring biomarkers; in fact, the developed device is not intended for quantitative assay, but is conceived as a compact, portable, user-friendly front-line screening tool usable for out-of-hospital self-diagnosis, with the additional gain of the possibility to carry out the data sharing and managing. A fundamental feature of the developed system consists in its high versatility and transversality, being the remote-controlled board suitable for all the sensing devices conceived for diagnostic purpose and based on the use of alkaline phosphatase as labelling enzyme.

The integration of IoT paradigm with innovative immunosensor based on nanostructured substrate allows for real-time availability of the test results to all interested subjects, ranging from the users to the clinicians. In respect to other solutions previously reported in literature [18], our device does not require custom changes in the reading hardware, as well as dedicated apps or specific features of the device's operating system. On the basis of the excellent performance obtained with the diagnosis of CD, used as case of study, our system paves the way for the use of IoT-WiFi architecture for a wide range of biomedical devices suitable for diagnostic and point of care applications.

References

- [1] E. Borgia, The Internet of Things vision: Key features, applications and open issues, *Comput. Commun.* 54 (2014),1-31.
- [2] N. Fernando, S. W. Loke, W. Rahayu, Mobile cloud computing: A survey, *Future Gener. Comput. Syst.* 29 (2013), 84-106.
- [3] P. Kassal, M. D. Steinberg, I. Murković Steinberg, Wireless chemical sensors and biosensors: A review, *Sensor Actuat. B-Chem*, 266 (2018), 228-245.
- [4] P. Wu, G. Vazquez, N. Mikstas, S. Krishnan and U. Kim, Aquasift: A low-cost, hand-held potentiostat for point-of-use electrochemical detection of contaminants in drinking water, 2017 IEEE Global Humanitarian Technology Conference (GHTC), San Jose, CA, 2017, pp. 1-4.
- [5] P. Oikonomou, A. Botsialas, A. Olziersky, I. Kazas, I. Stratakos, S. Katsikas, D. Dimas, K. Mermikli, G. Sotiropoulos, D. Goustouridis, I. Raptis, M. Sanopoulou, A wireless sensing system for monitoring the workplace environment of an industrial installation, *Sensor Actuat. B-Chem.* 224 (2016), 266-274.
- [6] M. D. Steinberg, P. Kassal, B. Tkalčec, I. Murković Steinberg, Miniaturised wireless smart tag for optical chemical analysis applications, *Talanta* 118 (2014), 375-381.

- [7] R. A. Potyrailo, N. Nagraj, C. Surman, H. Boudries, H. Lai, J. M. Slocik, N. Kelley-Loughnane, R. R. Naik, Wireless sensors and sensor networks for homeland security applications, *TrAC Trend Anal. Chem.* 40 (2012), 133-145.
- [8] W. Dang, L. Manjakkal, W. Taube Navaraj, L. Lorenzelli, V. Vinciguerra, R. Dahiya, Stretchable wireless system for sweat pH monitoring, *Biosens. Bioelectron.* 107 (2018), 192-202.
- [9] A. F. D. Cruz, N. Norena, A. Kaushik, S. Bhansali, A low-cost miniaturized potentiostat for point-of-care diagnosis, *Biosens. Bioelectron.* 62 (2014) 249-254.
- [10] J. Kim, S. Imani, W.R. de Araujo, J. Warchall, G. Valdés-Ramírez, T.R.L.C. Paixão, P.P. Mercier, J. Wang, Wearable salivary uric acid mouthguard biosensor with integrated wireless electronics, *Biosens. Bioelectron.* 74 (2015) 1061-1068.
- [11] A.J. Bandonkar, S. Imani, R. Nuñez-Flores, R. Kumar, C. Wang, A.M.V. Mohan, J. Wang, P.P. Mercier, Re-usable electrochemical glucose sensors integrated into a smartphone platform, *Biosens. Bioelectron.* 101 (2018) 181-187.
- [12] G. Xu, Q. Zhang, Y. Lu, L. Liu, D. Ji, S. Li, Q. Liu, Passive and wireless near field communication tag sensors for biochemical sensing with smartphone, *Sensor Actuat. B-Chem.* 246 (2017), 748-755.
- [13] M. D. Steinberg, P. Kassal, I. Kereković, I. Murković Steinberg, A wireless potentiostat for mobile chemical sensing and biosensing, *Talanta* 143 (2015), 178-183.
- [14] K. V. S. Rao, An overview of backscattered radio frequency identification system (RFID), *Microwave Conference, 1999 Asia Pacific, 1999*, pp. 746-749 vol.3.
- [15] S. Ortiz, Is near-field communication close to success?, *Computer*, 39.3 (2006),18-20.
- [16] V. Valente, M. Schormans and A. Demosthenous, An Energy-Efficient 1.2V 4-Channel Wireless CMOS Potentiostat for Amperometric Biosensors, 2018 IEEE International Symposium on Circuits and Systems (ISCAS), Florence, Italy, 2018, pp. 1-4.

- [17] G. F. Giordano, M. B.R. Vicentini, R. C. Murer, F. Augusto, M. F. Ferrão, G. A. Helfer, A. B. da Costa, A. L. Gobbi, L. W. Hantao, R. S. Lima, Point-of-use electroanalytical platform based on homemade potentiostat and smartphone for multivariate data processing, *Electrochim. Acta* 219 (2016), 170-177.
- [18] M. Bassoli, V. Bianchi, I. De Munari, P. Ciampolini, An IoT approach for an AAL Wi-Fi behavioral monitoring system, *IEEE Trans. on Instrum. and Meas.* 66.12 (2017) 3200-3209.
- [19] H. Maecker, T.M. Lindstrom, W.H. Robinson, P.J. Utz, M. Hale, S.D. Boyd, New tools for classification and monitoring of autoimmune diseases, *Nat. Rev. Rheumatol* 8.6 (2012) 317–328.
- [20] M. Giannetto, M. Mattarozzi, E. Umiltà, A. Manfredi, S. Quaglia, M. Careri, An amperometric immunosensor for diagnosis of celiac disease based on covalent immobilization of open conformation tissue transglutaminase for determination of anti-tTG antibodies in human serum, *Biosens. Bioelectron.* 62 (2014) 325-330
- [21] Eurachem Guide: The Fitness for Purpose of Analytical Methods – A Laboratory Guide to Method Validation and Related Topics, second ed., 2014. Available from <http://www.eurachem.org>
- [22] F. Bianchi, M. Careri, Experimental Design Techniques for Optimization of Analytical Methods. Part II: Spectroscopic and Electroanalytical Techniques, *Curr. Anal. Chem.* 4.2 (2008) 142–151
- [23] LMP91000 datasheet. Available at <http://www.ti.com/lit/ds/symlink/lmp91000.pdf>. Retrieved: Feb 27th, 2018.
- [24] Launchpad board datasheet. Available at <http://www.ti.com/tool/cc3200-launchxl#Technical Documents>. Retrieved: Feb 27th, 2018.

An integrated IoT-Wi-Fi board for remote data acquisition and sharing from innovative immunosensors. Case of study: diagnosis of celiac disease

Marco Giannetto^{a}, Valentina Bianchi^{b*}, Silvia Gentili^a, Simone Fortunati^a, Ilaria De Munari^b, Maria Careri^a*

^a Dipartimento di Scienze Chimiche, della Vita e della Sostenibilità Ambientale, Università di Parma. Parco Area delle Scienze 17/A, 43124 Parma (Italy)

^b Dipartimento di Ingegneria e Architettura, Università di Parma. Parco Area delle Scienze 181/A, 43124 Parma (Italy)

**Corresponding Authors:*

Marco Giannetto (marco.giannetto@unipr.it); Valentina Bianchi (valentina.bianchi@unipr.it)

Abstract

A new compact diagnostic device exploiting the integration of screen printed electrode-based immunosensors and remote-controlled IoT-WiFi acquisition board has been realized and validated for diagnosis of Celiac Disease as case of study. The immunodevice is based on chemisorption of open tissue transglutaminase enzyme on the surface of gold nanoparticles-functionalized carbon screen printed electrodes. IgA and IgG anti-tissue transglutaminase target antibodies are recognized by the immobilized bioreceptor as highly specific biomarkers related to Celiac Disease. The signal from the amperometric sensor is acquired and processed through on-purpose developed IoT-WiFi integrated board, allowing for real-time data sharing on cloud services to directly notify all users (physicians, caregivers, etc.) on device outcome. The proposed solution does not require customized hardware or software.

The analytical performances of the immunosensors were optimized by experimental design, obtaining diagnostically useful limit of detection (LOD) and limit of quantitation (LOQ)

values ($\text{LOD}_{\text{IgA}} = 3.2 \text{ AU mL}^{-1}$; $\text{LOD}_{\text{IgG}} = 1.4 \text{ AU mL}^{-1}$; $\text{LOQ}_{\text{IgA}} = 4.6 \text{ AU mL}^{-1}$; $\text{LOQ}_{\text{IgG}} = 2.3 \text{ AU mL}^{-1}$) as well as good intermediate precision ($\text{RSD} < 5\%$).

The high discrimination capability of the IoT-Wi-Fi **system device** between positive and negative serum control resulted to be suitable for diagnostic purposes, with outstanding statistical significance ($p < 0,001$)

1. Introduction

Wi-Fi infrastructures are nowadays highly diffused in the home context thanks to the comfort (or the need) to have a wireless gate to Internet. This wireless technology appears to be the most suitable for developing portable and connected devices usable autonomously by the user at home. In fact, Wi-Fi data transmission allows to take advantage of the infrastructure already present in the home environment or can be based on off-the-shelf solutions (e.g. standard modem/router) to ensure the connectivity to a diagnostic device, for example. This vision perfectly fits with the paradigm of the Internet of Things (IoT) [1]: in such a context, a sensor becomes an IoT node capable to acquire and send data independently but, at the same time, cooperating with other sensing devices, thus exploiting a maximally open network. Using this infrastructure, the data can be straightforwardly sent to a cloud platform and here processed [2].

Currently, wireless chemical sensors and biosensors are attracting a great deal of interest [3]. In fact, wireless technology simplifies the system architecture and improves the ease-of-operation of the device with respect to wired solutions [4]. Combining advances in wireless technology and chemical sensing has led to the development of devices with application in different fields [5-7]: among these, health care is of particular importance [8]. In addition, the application of the IoT vision to wireless chemical sensors designed for this application further increases the relevance of such devices. ~~Since~~ Nowadays cloud services allow to send messages (e.g. text messages, tweets, etc.), this feature can be exploited to send the diagnostic data directly on the phone/pc of the user/physician, without the necessity of developing custom apps, which represent an advantage with

respect to other solutions presented in literature [9,10]. Some of them are based on smartphones with dedicated adaptors [11-13]. For instance, Xu et al. [12] and Steinberg et al. [13] presented a RFID/NFC solution. Because of the peculiarities of the communication protocols involved, this solution requires the availability of a smartphone or a gateway at a very short distance [14,15]: the smartphone becomes actually a part of the data acquisition system, thus reducing the advantage in terms of cost and size of the overall system. Very recently, a wireless potentiostat, based on a novel low-complexity wireless unit exploiting a short-range inductive telemetry was presented [16]. Also in this case an Internet gateway would be mandatory in real world use, thus complicating the system architecture. A point-of-use platform for multivariate analyses based on the use of a potentiostat exploiting Bluetooth connectivity was reported: complex and multivariate data can be locally processed with a dedicated app or can be forwarded to a cloud service exploiting the smartphone connection [17]. Compared to these solutions, the integration of Wi-Fi and the IoT paradigm allows to exploit a unique hardware platform and a direct connection to the Internet without the need of a gateway, reducing the complexity of the system architecture, and therefore the costs associated with it, and improving ease-of-use.

Wi-Fi protocol has a well-known disadvantage with respect to other wireless standard, such as Bluetooth Low Energy (BLE) or ZigBee, regarding a higher power consumption: this could be overcome by some low-power design strategies. It has been proved that by adjusting the radio activity period it is possible to obtain excellent performances in terms of battery life for devices developed to transmit data with high frequency (e.g. environmental or personal data logger) [18]. In the case of chemical sensing devices, the frequency of data transmission is certainly much lower, so this problem is mitigated.

It is worth noting that these miniaturized portable devices will not have the same processing capabilities and measurement resolution of traditional benchtop instruments: however, the purpose of these devices is to provide an indication of occurrence of a particular disease-related biomarker and in some cases to address the user to further medical examination rather than to carry out an

accurate measurement. In this context, the target of the assay is the discrimination between positive (sick) and negative (healthy) samples.

Data gathered from diagnostic sensors can be locally processed and then transmitted over the Internet: this allows for a remote control of the user's health status. The idea behind is that of *online* monitoring: the adoption of technological solutions allows for follow-up of patients in their own homes without the need for constant interaction with a physician, and, in some cases, for building a database of parameters related to a particular pathology that can be useful for analyzing related statistics.

Electrochemical immunosensors represent a powerful tool for domiciliary self-diagnosis, as they require low-cost and simplified instrumentation that can be miniaturized in order to develop portable devices.

The peculiarities of immunosensors rely in shorter analysis time and in the possibility to perform quantitative or semi-quantitative analyses not limited to simple qualitative screening usually associated to conventional immunochemical approaches such as Enzyme Linked Immunosorbent Assay (ELISA) methods. Currently an increasing interest is focused on the application of these devices to diagnosis and monitoring of autoimmune diseases [19]. Among these, Celiac Disease (CD), showed in the last decades a more and more frequent occurrence. For this reason, the discovery of new reliable biomarkers had as a consequence the development of high-performance immunosensors devoted to detection/quantification of specific CD-related biomarkers.

CD occurs in genetically predisposed individuals as a result of ingestion of gluten, the protein component of cereals such as wheat, rye, etc. CD is characterized by an immune response triggered by the recognition of gliadin peptides, the alcohol-soluble component of gluten, along with an increase of T-lymphocytes in the intestinal mucosa. This results in inflammatory processes and spoilage of the latter, examined via duodenal biopsy, together with the expression of specific antibodies proved to be disease-related biomarkers. Among these, the anti-tissue transglutaminase antibodies (anti-tTG) directed versus the open conformation of transglutaminase enzyme can be

determined and monitored via hematic assays, both in the IgG (gamma-immunoglobulines) and IgA (alpha-immunoglobulines) forms to avoid false negative responses associated with IgA deficiency.

In this scenario, an amperometric immunosensor based on covalent immobilization of the enzymatic receptor (Open tTG[®]) in its open conformation for the determination of antibodies anti-tTG has been recently developed by our research group [20].

In such a context, the aim of the present study was to realize and validate a compact diagnostic device and to optimize the previously cited amperometric immunosensor in order to fit the new IoT-Wi-Fi based diagnostic tool. The immunodevice is based on the direct chemisorption of Open tTG[®] on the surface of Gold NanoParticles-functionalized Carbon Screen Printed Electrodes (GNP-CSPEs). Anti-tTG target antibodies are recognized from the immobilized bioreceptor and subsequently detected through alkaline phosphatase-labelled anti-human IgA/IgG.

The so modified GNP-CSPEs are then connected to the newly developed IoT-Wi-Fi board for remote data acquisition. The measurements are then processed and transmitted through a standard Wi-Fi connection and stored in an open cloud platform. Details about the hardware and the software solutions are given in the experimental section.

2. Experimental

2.1. Materials

Trizma[®] base, ethylenediaminetetraacetic acid disodium salt dihydrate (Na₂EDTA), DL-dithiothreitol (DTT), sodium chloride (NaCl), calcium dichloride hexahydrate (CaCl₂·6H₂O), albumin from bovine serum (BSA), magnesium chloride anhydrous (MgCl₂), Tween[®] 20 and human serum were purchased from Sigma-Aldrich (Milan, Italy). Hydroquinone diphosphate (HQDP) was from Metrohm Italiana (DropSens DRP-HQDP) (Origgio, Italy).

Double-distilled and deionized water purified with a Milli-Q system was used for the preparation of the buffered solutions.

“Enzyme buffer” (EB) was prepared according to the following composition: 0.02 M Trizma® base, 0.001 M Na₂EDTA, 0.001 M DTT, 0.15 M NaCl, 0.01 M CaCl₂·6H₂O (pH 7.2). Tris buffered saline (TBS) was prepared according to the following composition: 0.1 M Trizma® base, 0.02 M MgCl₂ (pH 7.4). “Sample buffer” (SB) and “wash buffer” (10×) were contained in ELISA kits. Diluted “wash buffer” (WB 1×) was prepared by dilution of “wash buffer” 10× in water. “Reading buffer” (RB) was prepared according to the following composition: 0.1 M Trizma® base, 0.02 M MgCl₂ (pH 9.8).

Human tissue transglutaminase stabilized in its open conformation (Open tTG[®]) was supplied from Zedira (Darmstadt, Germany). In order to maintain the open conformation, working solutions of open-tTG were prepared in EB. ZediXclusive Open tTG[®]-Ab (IgA) and ZediXclusive Open tTG[®]-Ab (IgG) ELISA kits were purchased from Zedira. Each kit contained six calibrator solutions of anti-tTG antibodies (0, 1, 3, 10, 30, 100 AU mL⁻¹) and a positive and a negative control. For the assessment of unknown samples, the kits’ instructions established normal (negative) range (< 2.6 AU mL⁻¹), threshold value (3.0 AU mL⁻¹), equivocal range (2.6-3.5 AU mL⁻¹) and positive range (> 3.5 AU mL⁻¹). Alkaline phosphatase-labelled rabbit anti-human immunoglobulins IgA (anti-H-IgA-AP) and IgG (anti-H-IgG-AP) were from Sigma-Aldrich. Open tTG[®], anti-H-IgA-AP and anti-H-IgG-AP were aliquoted and stored at -20 °C after delivery.

Interference studies were performed by using ZediXclusive DGPx1-ab (IgA) and ZediXclusive DGPx1-ab (IgG) ELISA kits ~~were~~ purchased from Zedira GmbH (Darmstadt, Germany).

2.2. Instrumentation

Immunosensors were assembled on GNP-CSPEs purchased by Metrohm Italiana (DropSens DRP-110GNP) (Origgio, Italy).

All electrochemical measurements were performed with a μ Autolab III electrochemical workstation (EcoChemie, Utrecht, NL) equipped with GPES 4.9 version customized software and connected to DropSens DRP-DSC plug.

2.3. Immunosensor set-up

In order to perform the enzyme covalent linking, the GNP electrodes were incubated for 3 h at room temperature with 25 μ L of open-tTG solution, properly diluted (see section 3.1) in EB from the original stock solution. After removal of unreacted enzyme by accurate washing with EB, a blocking treatment, aimed at preventing unspecific responses during sample incubation, was carried out by casting 50 μ L of a 20 mg mL⁻¹ solution of BSA dissolved in EB on each electrode for an incubation time of 60 min, followed by washing with the same buffer. The ready to use GNP/Open-tTG modified electrodes were dried and stored at 4 °C when not in use.

Detection of anti-tTG antibodies was carried out by incubating the immunosensors with 20 μ L of sample (standard solutions from ELISA kits or 1:100 diluted human serum) for 60 min. The sensors were then carefully washed with WB and finally with TBS in order to prevent unspecific binding phenomena. Subsequently, each immunosensor was incubated for 60 min with 50 μ L of anti-H-IgA-AP or anti-H-IgG-AP, diluted in SB as described in section 3.1, in order to reveal anti-tTG antibodies previously immobilized on the electrodic surface. The protocol implemented for the realization of the immunosensors is schematically represented in Scheme 1: after direct chemisorption of the tTG enzyme on the electrodic surface, a blocking with BSA was carried out. Under these conditions the sensor is ready to be stocked until use, consisting in incubation of the sensing surface with the 1:100-diluted serum sample, followed by incubation with AP-conjugated

anti-H-IgA or -IgG and amperometric reading of the assay. The reading of the electrochemical immunoassay was performed by Differential Pulse voltammetry (DPV) measurements using 50 μL of a 1 mg mL^{-1} solution of HQDP dissolved in RB. DPV curves were acquired by scanning the potential between -0.5 V and +0.3 V (step potential= +0.00495 V, modulation amplitude= +0.04995 V, modulation time= 0.102 s, interval time= 0.4 s) and recording the signal ascribable to the oxidation of hydroquinone HQ, generated by AP-promoted enzymatic dephosphorylation of HQDP, to Quinone (Q). The peak current is associated with the amount of produced HQ, which is related to the concentration of the immobilized anti-H-IgA (or IgG)-AP. The amount of immunosorbed anti-H-IgA (or IgG)-AP is finally related to the concentration of the anti-tTG target antibodies in the incubated sample. At least three replicate measurements were carried out for all standards and samples. Intermediate precision was obtained performing three replicated measurements for each concentration levels on independently fabricated immunosensors.

Method validation was performed by calculating limit of detection (LOD) and limit of quantification (LOQ) according to “Eurachem Guidelines” [21].

2.4. Experimental design

The experimental response was optimized in terms of P/N ratio (P=positive control; N=negative control) in order to assess the best concentrations of *i*) the Open tTG[®] solution used for the immobilization of the enzymatic receptor and *ii*) of the reading anti-H-IgA(or IgG)-AP antibodies. Previously, ANOVA tests were carried out with the aim of assessing the significance of factors subjected to optimization by means of a 3² three-levels Full Factorial Design (FFD) [22]. Each of the nine experiments was replicated three times and acquired under randomized sequence. All statistical calculations were performed using the Statgraphics software package (Statgraphics Technologies Inc., Virginia, USA).

2.5. IoT Wi-Fi Acquisition System Device

The acquisition system consists of two parts: an analog front-end (AFE) and a data acquisition and processing unit. The AFE is based on the integrated potentiostat LMP91000, for the cell conditioning and current detection resulting from the enzyme reaction occurring on GNP-CSPEs. The AFE is connected to a Wi-Fi based System on Chip (CC3200) for data sampling, processing and transmission. For preliminary tests, a prototypal sensor based on LMP91000 and CC3200 development boards was designed. The whole system is shown in Figure 1.

The prototype dimensions ($18 \times 5.7 \times 2.7$ cm), although conditioned by those of the development boards, are definitely reduced compared to a traditional acquisition system. Further reduced size is expected in the engineered version.

In the following subsections both AFE and Microcontroller Unit (MCU) are described and detailed.

2.5.1. Analog Front End

To read the electrochemical signal from the cell implemented on GNP-CSPEs, a potentiostat performing DPV scans was exploited: for this purpose the LMP91000 [23], an integrated potentiostat by Texas Instruments, was used (Figure 2).

This circuit can be programmed through an I2C interface to generate an appropriate bias voltage (V_{bias}), applied between the control (V_{ce}) and reference (V_{re}) electrodes, capable of conditioning the cell. V_{bias} , in the present case of study related to the novel immunosensor for anti-tTG antibodies determination, should range from -0.6V to 0.5V. The LMP91000 allows to select up to 27 discrete voltage levels for the bias signal. These levels are defined as a percentage of a voltage reference V_{ref} : the LMP91000 allows the selection between an internal reference (3.3V) or a custom external one. The internal reference was selected allowing to achieve the desired span without adding other components. In order to have negative values for V_{bias} , V_{ref} should have a strictly positive value. In

LMP91000 V_{ce} , can be programmed as 20%, 50% or 67% in respect to V_{ref} . It is worth to note also that, since the potentiostat has a single supply voltage circuitry, V_{ce} , V_{re} , V_{we} and V_{out} must be equal or major than zero: this imply that the following relationship should be verified

$$V_{ce} \geq V_{bias}$$

With the given voltage range, all values that is possible to program in the LMP91000 are compatible with the equation above. A value of 0.66V corresponding at 20% of V_{ref} was selected: this permits to maintain the voltages in a range directly compatible with the inputs of the MCU module, as described below, removing the need of a dedicated interface circuitry.

Once defined V_{ref} and V_{ce} , a bias signal was generated using the maximum possible number of levels to achieve the maximum resolution in reading the cell. In particular, starting from a -24% of the V_{ref} , 34 levels were considered, according to the Figure 3, to obtain exactly the desired range.

2.5.2. IoT Wi-Fi Module

The system-on-chip CC3200 by Texas Instruments was chosen for the device core. This SoC integrates an MCU with an ARM Cortex-M4 architecture and a network processor compliant with the IEEE 802.11b/g/n network protocol radio. This makes the whole system Wi-Fi certified.

The CC3200 is mounted on a development board (LaunchPadXL board [24]) that was used as a motherboard to develop the first version of the acquisition system. The working and reference electrodes and V_{out} pins from the LMP91000 board are connected to Analog to Digital inputs of the CC3200. Since the ADC inputs can manage voltages below 1.4V, and all the resulting voltage are in this range, there is no need of an interface between the two boards.

In the present study a cloud-based framework was adopted in order to allow for remote monitoring. The system “intelligence” can be distributed among the sensing device themselves (“smart” object), and external, cloud-based services. For prototypal purposes, data elaboration was performed directly on the cloud platform, but the same operations can be carried out also directly on the MCU,

without any change in the result but lowering the battery consumption of the whole device thanks to the limitation of the energy hungry Wi-Fi transmission phases. In Figure 4, a generic architecture is shown. The data flowing from the end device go straightforwardly through the modem/router via Wi-Fi Protected Access (WPA) standard protocol to be stored and processed in the Internet cloud. The wide coverage of Wi-Fi router makes easier to ensure stable sensor connection over a large area. Once delivered to the cloud, sensor data are stored and subsequently processed, in order to extract meaningful information. The sensor can be connected straightforwardly to different cloud environment by suitably coding the access method into the device firmware. The cloud environment also hosts a full set of analytical functions and converting raw sensor data into accessible information. Both raw data and synthesized analytics outcomes are then accessible through the cloud methods. In the present work an IoT open platform Thinkspeak©, which is a cloud platform supporting MATLAB data analytics, was adopted. The choice of this platform is not binding, but any other cloud platform (e.g. IBM Bluemix, Microsoft Azure etc), can be exploited as well. In Thinkspeak, using Representational State Transfer (REST) Application Programming Interface (API), it is possible to create and modify channels in which store the data for the subsequent elaboration. Details about the signal processing and elaboration are given in section 2.6.

2.6. Signal processing

The measured voltages are then processed to extrapolate the cell current due to the chemical reaction.

A current value is calculated for each point of the bias signal following the equation

$$I = \frac{V_{out} - V_w}{G}$$

where V_{out} is the LMP91000 output voltage (Figure 2), V_w is the reference voltage and G is the programmable TransImpedance Amplifier (TIA) gain. For the TIA gain a value of 7000 was

selected to avoid signal saturation. To detect a positive diagnosed user or to a negative one, the value of the peak of the current computed as the difference between the current on the bias signal (V_{bias}) rising edge and that on the falling edge has to be evaluated. This leads to 17 measurement points for each acquisition. It has to be noticed that the number of acquisition points is considerably lower to that obtainable from bench-top instruments: as already mentioned, however, this resolution is perfectly compatible with the discrimination of the disease-positive users and the negative ones, as will be demonstrated subsequently. In Figure 5 an example of measured bias signal and currents is given.

As the baseline of the differential current (baseline drift) is frequently not perfectly parallel to the x-axis, it is not possible to apply simple methods for searching the maximum to evaluate the amplitude of the peak in the obtained current waveform. For this purpose, before peak evaluation, a baseline search and calculation algorithm was introduced for each measurement. Four absolute minimum points were identified for each waveform and a baseline was estimated using a linear polynomial fitting. This baseline is then used as a reference to calculate the actual peak amplitude, as shown in Figure 6.

3. Results and discussion

3.1. Optimization of the response

In order to find the optimal concentration values of Open tTG[®] (factor 1) and anti-H-IgA-AP or anti-H-IgG-AP (factor 2), a 3² three-levels FFD was performed. Two independent experimental datasets were acquired for anti-tTG IgA and IgG, considering as response variable the P/N ratio, calculated from the peak current values related to positive (P) and negative (N) control samples. For detection of anti-tTG IgA antibodies the explored concentration levels of the Open tTG[®] were 4.58 $\mu\text{g mL}^{-1}$, 9.16 $\mu\text{g mL}^{-1}$, 18.32 $\mu\text{g mL}^{-1}$, whereas in the case of anti-tTG IgG the concentration set for Open tTG[®] was 9.16 $\mu\text{g mL}^{-1}$, 18.32 $\mu\text{g mL}^{-1}$, 45.8 $\mu\text{g mL}^{-1}$. As for the second optimized factor

(anti-H-IgA(or IgG)-AP antibodies) the explored concentration levels for anti-H-IgA-AP were 0.5 $\mu\text{g mL}^{-1}$, 1 $\mu\text{g mL}^{-1}$, 2 $\mu\text{g mL}^{-1}$, whereas for anti-H-IgG-AP concentrations ranged from 1 $\mu\text{g mL}^{-1}$ to 4 $\mu\text{g mL}^{-1}$.

The significance of the main effects and of their reciprocal interaction was checked by 2-way ANOVA with Bonferroni post hoc test. In the case of the determination of target anti-tTG IgA antibodies, both factors and their interaction resulted to be significant ($p < 0.001$). As for IgG antibodies, the Open tTG[®] concentration effect was significant with $p < 0.005$, whereas anti-H-IgG-AP antibodies and binary interaction effects were significant with $p < 0.001$.

The Open tTG[®] and anti-H-IgA-AP concentrations leading to an optimal P/N ratio for the determination of IgA anti-tTG antibodies were, respectively, 4.58 $\mu\text{g mL}^{-1}$ and 1 $\mu\text{g mL}^{-1}$, as deduced from the ANOVA interaction plot shown in Figure 7. Analogous experiments carried out for the determination of IgG anti-tTG antibodies gave concentrations of 9.16 $\mu\text{g mL}^{-1}$ and 1 $\mu\text{g mL}^{-1}$ as optimal respective values for Open tTG[®] and anti-H-IgG-AP, as from ANOVA interaction plot shown in Figure 8. Under these conditions the immunosensor was capable to quantify both IgA and IgG antibodies in a diagnostically useful concentration range.

3.2. Analytical performance

The immunosensor performance was evaluated for anti-tTG human IgA and IgG by incubation of the calibrating solutions included in the ELISA kits. Linearity of the response was checked over the 0-100 AU mL⁻¹ concentration range and assessed over the 0-30 AU mL⁻¹ range. As can be observed from the calibration functions reported in Figures 9 and 10, the best sensitivity was achieved in the case of anti-tTG human IgG. Accordingly, LOD values analytically useful for diagnostic purposes were 3.2 AU mL⁻¹ for IgA and 1.4 AU mL⁻¹ for IgG. LOQ values of 4.6 AU mL⁻¹ and 2.3 AU mL⁻¹ were calculated, respectively.

Concerning the intermediate precision of the measurements obtained using the sensors, good results were achieved, giving Relative Standard Deviation (%RSD) values <5% for both IgA and IgG anti-tTG.

3.3. Interference study

The specificity of the immunosensing device was assessed by interference studies carried out using anti-deamidated gliadin (DGPx1-Ab) human IgG and IgA antibodies, chosen as biomarkers potentially occurring in serum samples from subjects affected by Celiac Disease. In fact, although anti-tTG antibodies are currently considered as the most specific serological biomarkers associated to CD, anti-deamidated gliadin antibodies are frequently expressed, especially in pre-diagnostic stage, when the subject has not yet undertaken the gluten-free diet. For this purpose, we evaluated the response of the immunosensor to DGPx1-Ab both in presence and absence of anti-tTG. Negative serum controls spiked with DGPx1-Ab IgA and IgG at different concentrations (3, 18 and 100 U/mL; threshold value < 6.7 U/mL) showed in all cases current responses not significantly different ($p>0,05$) from non-spiked negative serum controls. Furthermore, anti-tTG-positive serum control spiked with DGPx1-Ab of both isotypes gave responses not significantly different ($p>0,05$) from the non-spiked positive serum controls, keeping the P/N ratio reported in section 3.1.

3.4. Acquisitions with the Iot-WiFi device

On the basis of the optimized experimental conditions assessed with the conventional instrumentation (potentiostat), additional datasets were acquired with the innovative IoT-WiFi device developed within this study, in order to test its performance. For this purpose, we acquired signals from 1:100 diluted positive and negative human serum controls. Selections of signals

recorded for anti-tTG IgA and IgG are reported in Figures 11 and 12, respectively (4 replicated acquisition for both positive and negative IgA and IgG serum controls).

The significance of the difference between positive and negative human serum controls was verified by 1-way ANOVA with Bonferroni post-hoc test, for the determination of both anti-tTG antibodies IgA and IgG. The negative and positive datasets resulted to be different with a very high significance level ($p < 0.001$)

The box-and-whiskers plots for IgA and IgG are reported in Figures 13 and 14.

4. Conclusions

The capability of the IoT-Wi-Fi device in terms of discrimination between positive and negative serum control resulted to be remarkable and suitable for diagnostic purpose, **also considering the specificity with respect to other potentially occurring biomarkers**; in fact, the developed device is not intended for quantitative assay, but is conceived as a compact, portable, user-friendly front-line screening tool usable for out-of-hospital self-diagnosis, with the additional gain of the possibility to carry out the data sharing and managing. A fundamental feature of the developed system consists in its high versatility and transversality, being the remote-controlled board suitable for all the sensing devices conceived for diagnostic purpose and based on the use of alkaline phosphatase as labelling enzyme.

The integration of IoT paradigm with innovative immunosensor based on nanostructured substrate allows for real-time availability of the test results to all interested subjects, ranging from the users to the clinicians. In respect to other solutions previously reported in literature [18], our device does not require custom changes in the reading hardware, as well as dedicated apps or specific features of the device's operating system. On the basis of the excellent performance obtained with the diagnosis of CD, used as case of study, our system paves the way for the use of IoT-WiFi architecture for a wide range of biomedical devices suitable for diagnostic and point of care applications.

References

- [1] E. Borgia, The Internet of Things vision: Key features, applications and open issues, *Comput. Commun.* 54 (2014),1-31.
- [2] N. Fernando, S. W. Loke, W. Rahayu, Mobile cloud computing: A survey, *Future Gener. Comput. Syst.* 29 (2013), 84-106.
- [3] P. Kassal, M. D. Steinberg, I. Murković Steinberg, Wireless chemical sensors and biosensors: A review, *Sensor Actuat. B-Chem*, 266 (2018), 228-245.
- [4] P. Wu, G. Vazquez, N. Mikstas, S. Krishnan and U. Kim, Aquasift: A low-cost, hand-held potentiostat for point-of-use electrochemical detection of contaminants in drinking water, 2017 IEEE Global Humanitarian Technology Conference (GHTC), San Jose, CA, 2017, pp. 1-4.
- [5] P. Oikonomou, A. Botsialas, A. Olziersky, I. Kazas, I. Stratakos, S. Katsikas, D. Dimas, K. Mermikli, G. Sotiropoulos, D. Goustouridis, I. Raptis, M. Sanopoulou, A wireless sensing system for monitoring the workplace environment of an industrial installation, *Sensor Actuat. B-Chem.* 224 (2016), 266-274.
- [6] M. D. Steinberg, P. Kassal, B. Tkalčec, I. Murković Steinberg, Miniaturised wireless smart tag for optical chemical analysis applications, *Talanta* 118 (2014), 375-381.

- [7] R. A. Potyrailo, N. Nagraj, C. Surman, H. Boudries, H. Lai, J. M. Slocik, N. Kelley-Loughnane, R. R. Naik, Wireless sensors and sensor networks for homeland security applications, *TrAC Trend Anal. Chem.* 40 (2012), 133-145.
- [8] W. Dang, L. Manjakkal, W. Taube Navaraj, L. Lorenzelli, V. Vinciguerra, R. Dahiya, Stretchable wireless system for sweat pH monitoring, *Biosens. Bioelectron.* 107 (2018), 192-202.
- [9] A. F. D. Cruz, N. Norena, A. Kaushik, S. Bhansali, A low-cost miniaturized potentiostat for point-of-care diagnosis, *Biosens. Bioelectron.* 62 (2014) 249-254.
- [10] J. Kim, S. Imani, W.R. de Araujo, J. Warchall, G. Valdés-Ramírez, T.R.L.C. Paixão, P.P. Mercier, J. Wang, Wearable salivary uric acid mouthguard biosensor with integrated wireless electronics, *Biosens. Bioelectron.* 74 (2015) 1061-1068.
- [11] A.J. Bandonkar, S. Imani, R. Nuñez-Flores, R. Kumar, C. Wang, A.M.V. Mohan, J. Wang, P.P. Mercier, Re-usable electrochemical glucose sensors integrated into a smartphone platform, *Biosens. Bioelectron.* 101 (2018) 181-187.
- [12] G. Xu, Q. Zhang, Y. Lu, L. Liu, D. Ji, S. Li, Q. Liu, Passive and wireless near field communication tag sensors for biochemical sensing with smartphone, *Sensor Actuat. B-Chem.* 246 (2017), 748-755.
- [13] M. D. Steinberg, P. Kassal, I. Kereković, I. Murković Steinberg, A wireless potentiostat for mobile chemical sensing and biosensing, *Talanta* 143 (2015), 178-183.
- [14] K. V. S. Rao, An overview of backscattered radio frequency identification system (RFID), *Microwave Conference, 1999 Asia Pacific, 1999*, pp. 746-749 vol.3.
- [15] S. Ortiz, Is near-field communication close to success?, *Computer*, 39.3 (2006),18-20.
- [16] V. Valente, M. Schormans and A. Demosthenous, An Energy-Efficient 1.2V 4-Channel Wireless CMOS Potentiostat for Amperometric Biosensors, 2018 IEEE International Symposium on Circuits and Systems (ISCAS), Florence, Italy, 2018, pp. 1-4.

- [17] G. F. Giordano, M. B.R. Vicentini, R. C. Murer, F. Augusto, M. F. Ferrão, G. A. Helfer, A. B. da Costa, A. L. Gobbi, L. W. Hantao, R. S. Lima, Point-of-use electroanalytical platform based on homemade potentiostat and smartphone for multivariate data processing, *Electrochim. Acta* 219 (2016), 170-177.
- [18] M. Bassoli, V. Bianchi, I. De Munari, P. Ciampolini, An IoT approach for an AAL Wi-Fi behavioral monitoring system, *IEEE Trans. on Instrum. and Meas.* 66.12 (2017) 3200-3209.
- [19] H. Maecker, T.M. Lindstrom, W.H. Robinson, P.J. Utz, M. Hale, S.D. Boyd, New tools for classification and monitoring of autoimmune diseases, *Nat. Rev. Rheumatol* 8.6 (2012) 317–328.
- [20] M. Giannetto, M. Mattarozzi, E. Umiltà, A. Manfredi, S. Quaglia, M. Careri, An amperometric immunosensor for diagnosis of celiac disease based on covalent immobilization of open conformation tissue transglutaminase for determination of anti-tTG antibodies in human serum, *Biosens. Bioelectron.* 62 (2014) 325-330
- [21] Eurachem Guide: The Fitness for Purpose of Analytical Methods – A Laboratory Guide to Method Validation and Related Topics, second ed., 2014. Available from <http://www.eurachem.org>
- [22] F. Bianchi, M. Careri, Experimental Design Techniques for Optimization of Analytical Methods. Part II: Spectroscopic and Electroanalytical Techniques, *Curr. Anal. Chem.* 4.2 (2008) 142–151
- [23] LMP91000 datasheet. Available at <http://www.ti.com/lit/ds/symlink/lmp91000.pdf>. Retrieved: Feb 27th, 2018.
- [24] Launchpad board datasheet. Available at <http://www.ti.com/tool/cc3200-launchxl#Technical Documents>. Retrieved: Feb 27th, 2018.

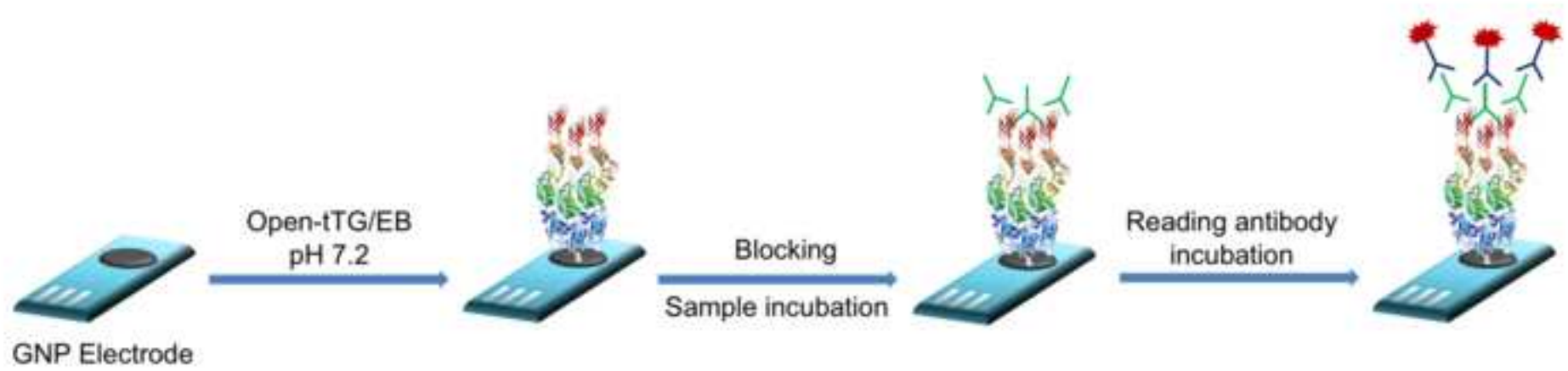


Figure 1
[Click here to download high resolution image](#)

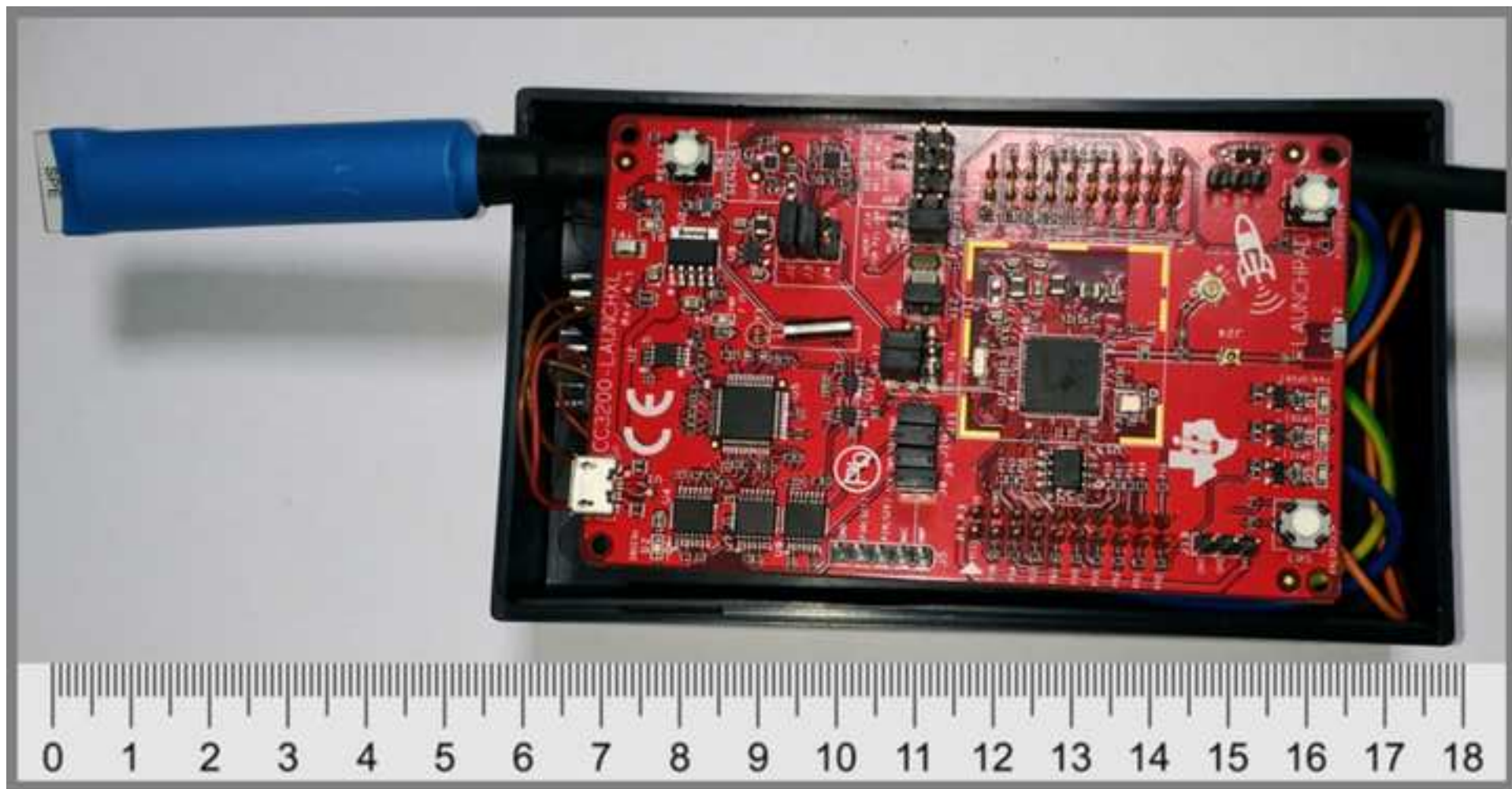


Figure 2

[Click here to download high resolution image](#)

IoT-WiFi device architecture

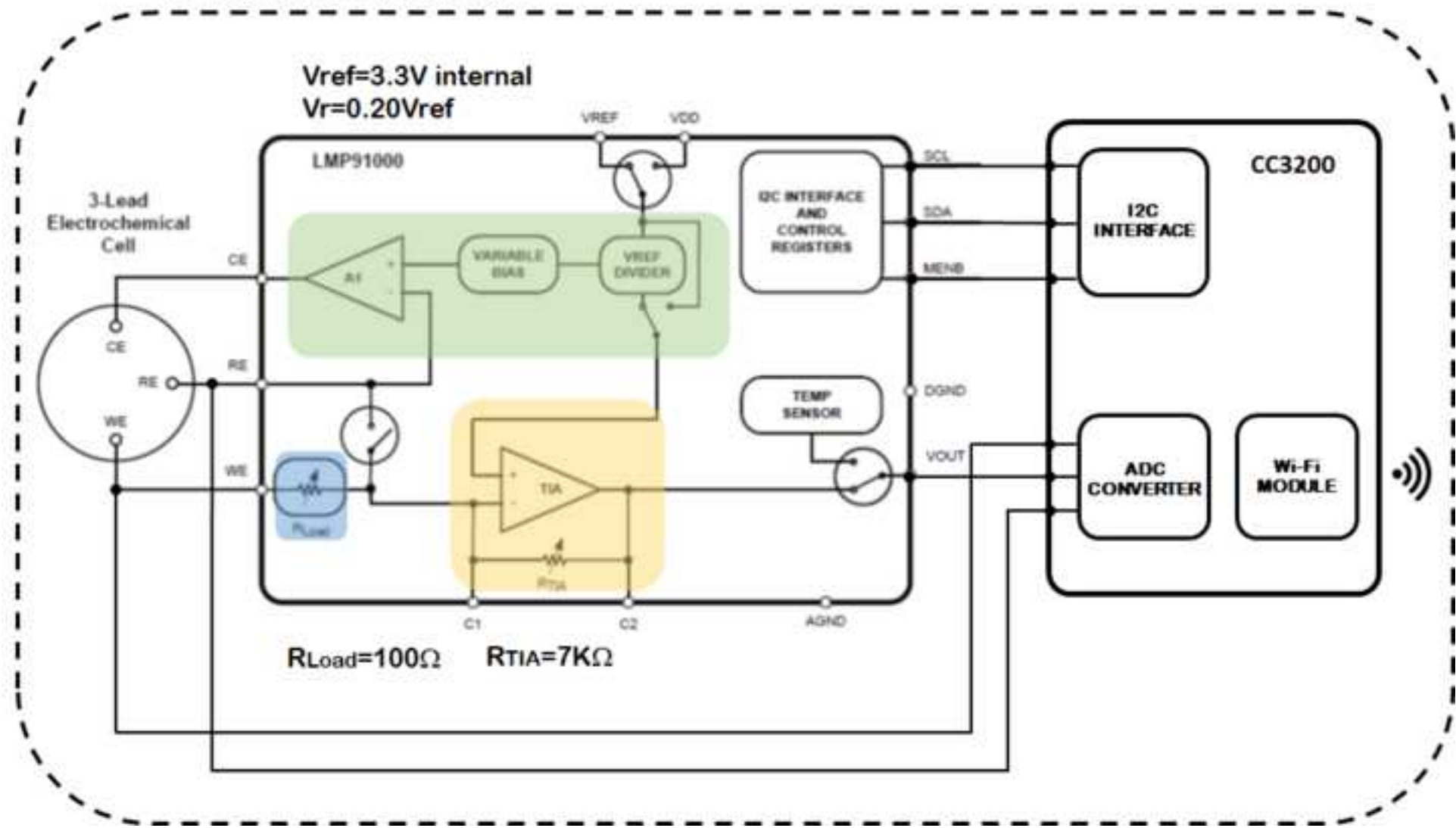


Figure 3
[Click here to download high resolution image](#)

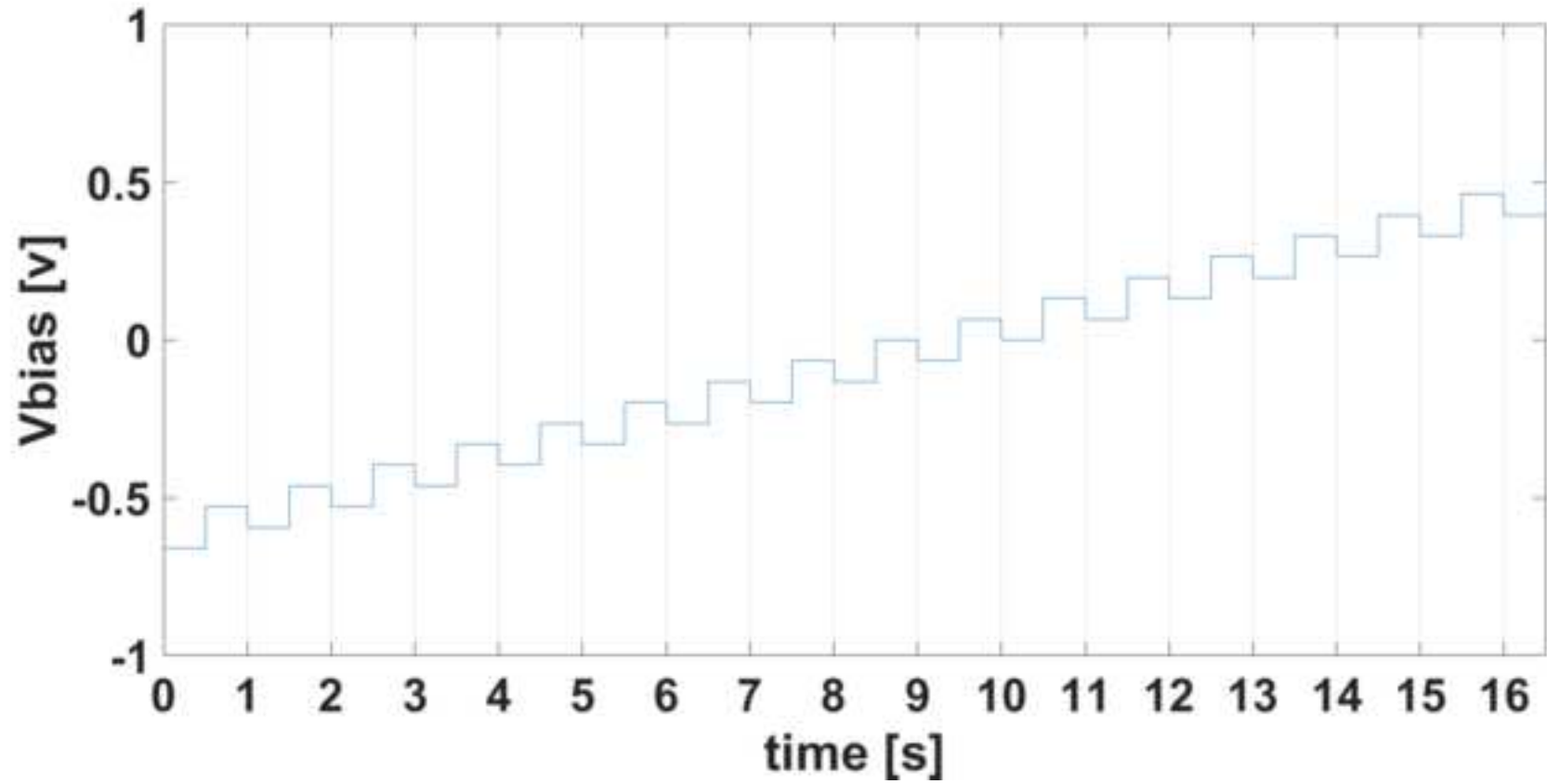


Figure 4
[Click here to download high resolution image](#)

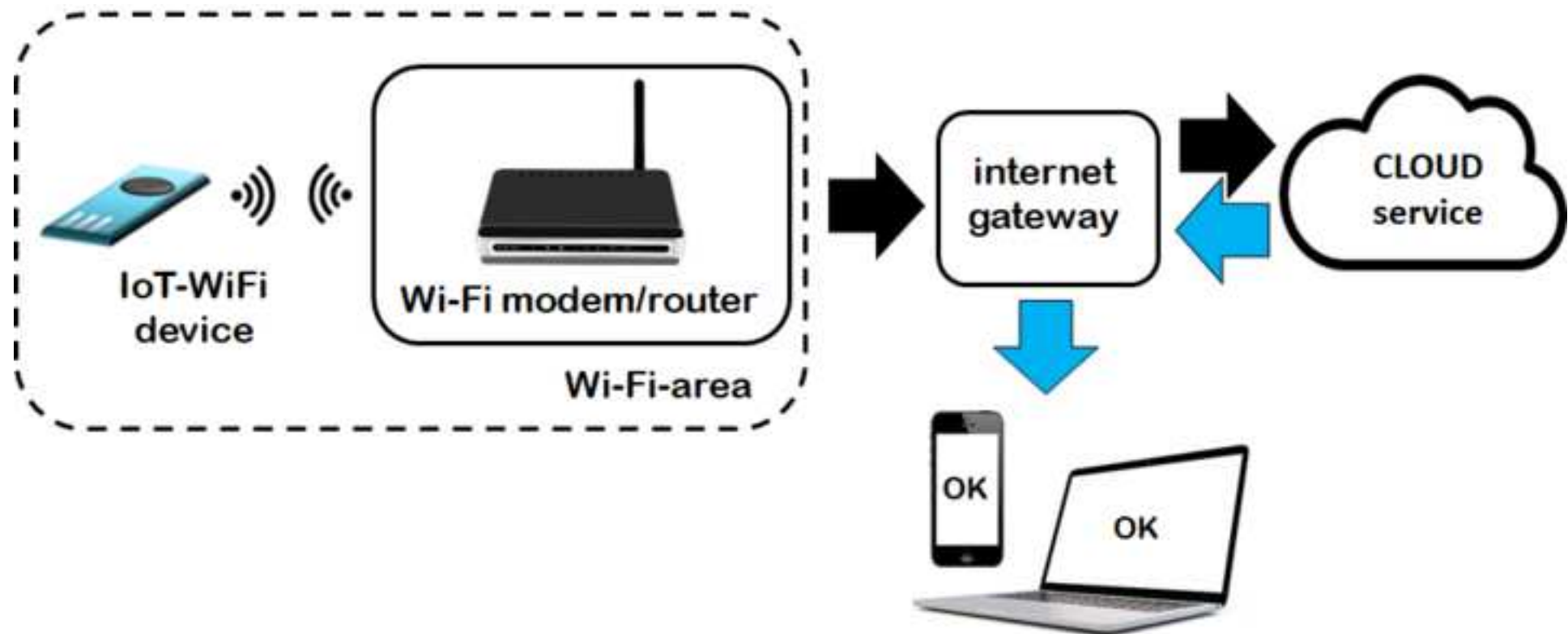


Figure 5
[Click here to download high resolution image](#)

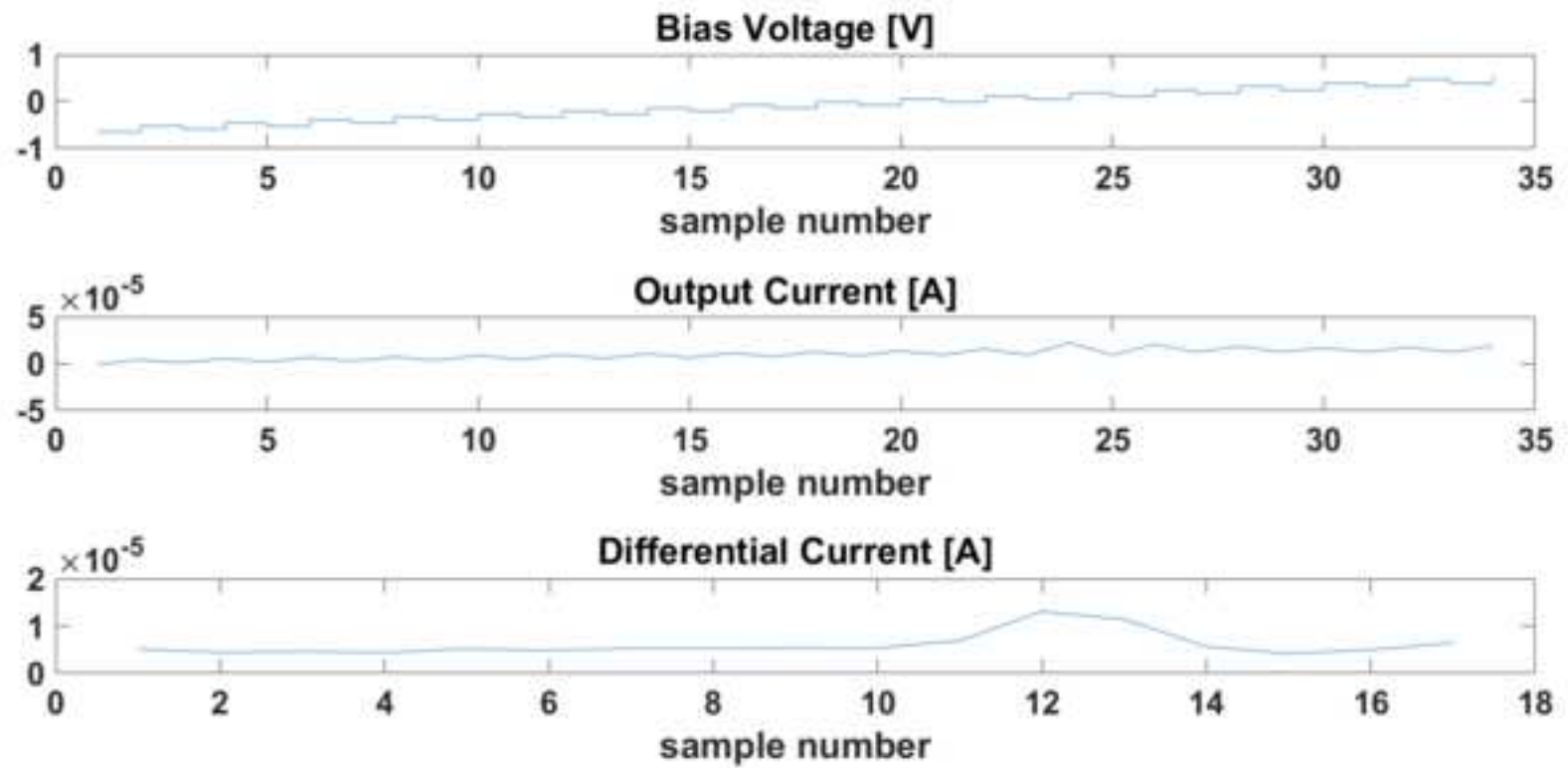


Figure 6
[Click here to download high resolution image](#)

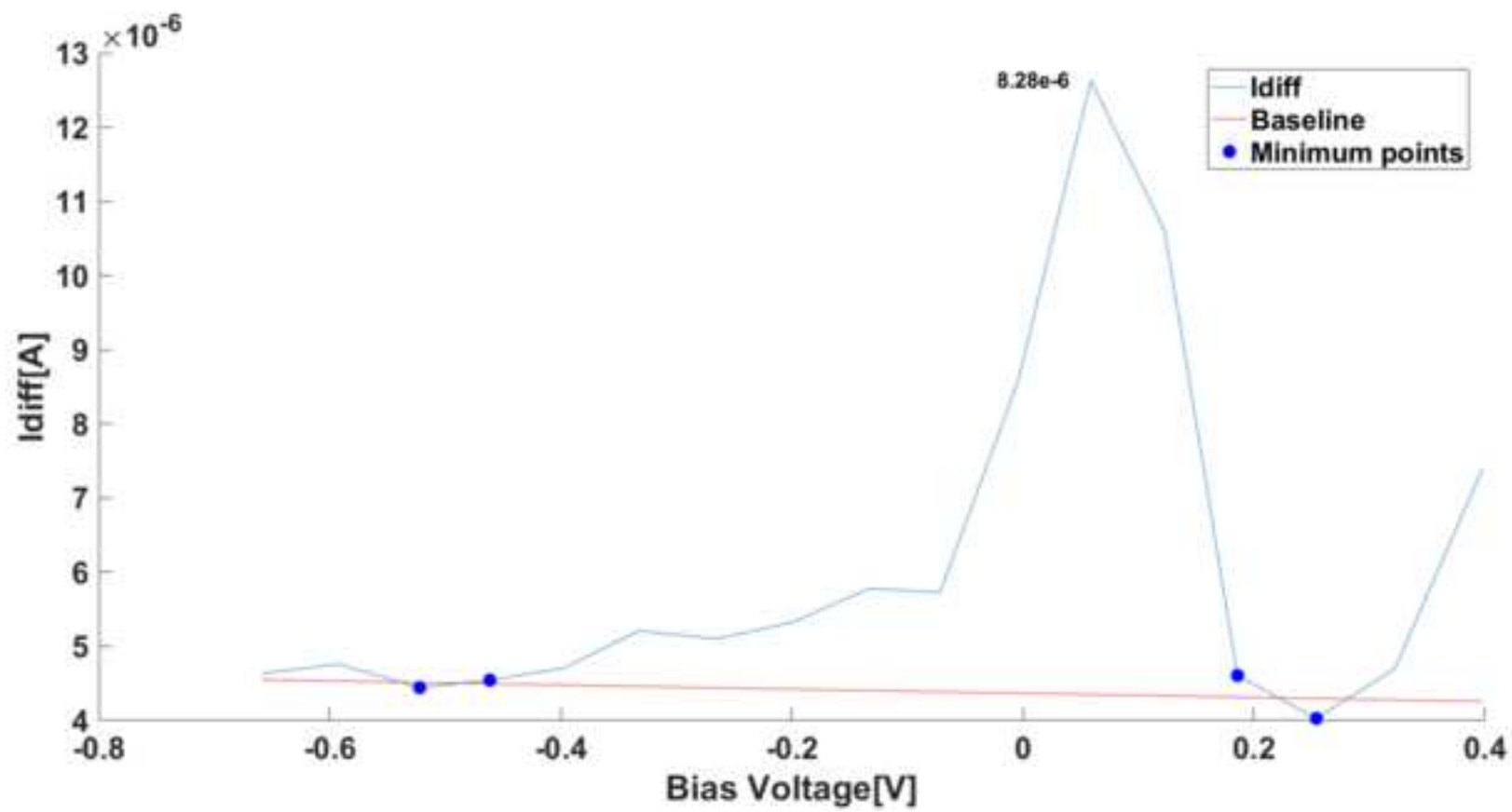


Figure 7
[Click here to download high resolution image](#)

Interactions and 95.0 Percent LSD Intervals

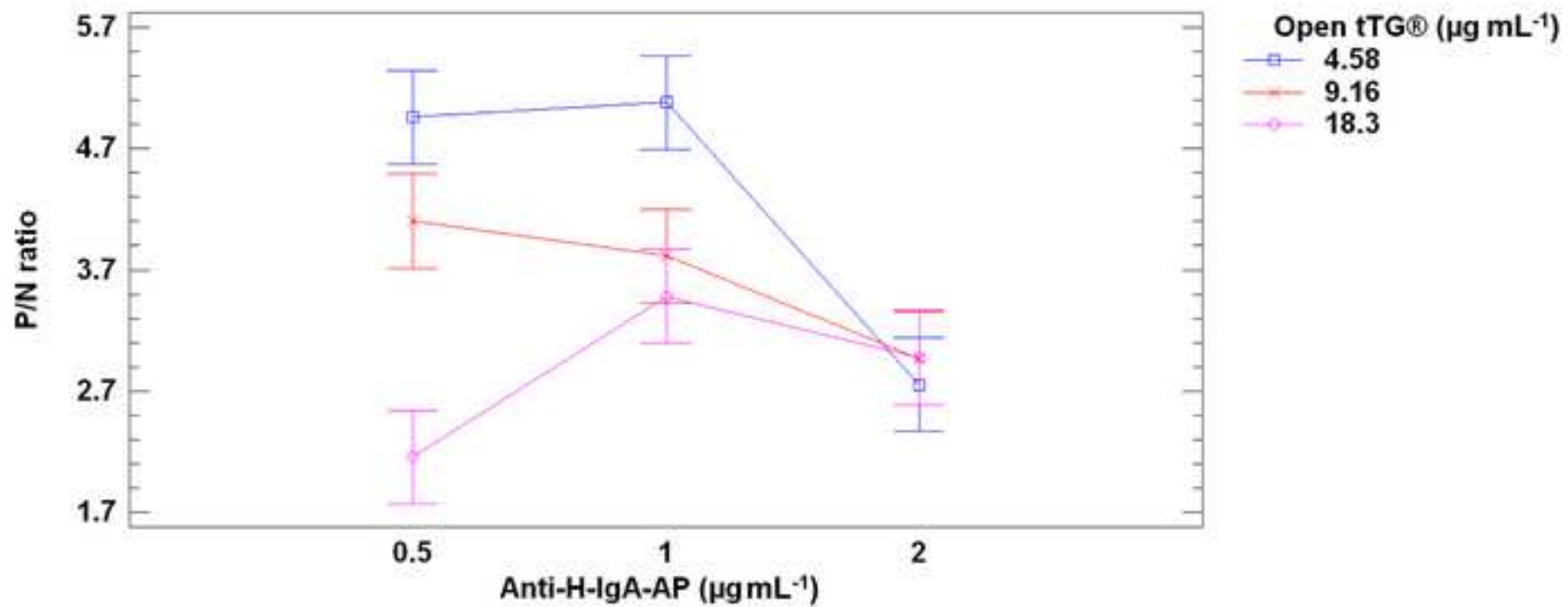


Figure 8
[Click here to download high resolution image](#)

Interactions and 95.0 Percent LSD Intervals

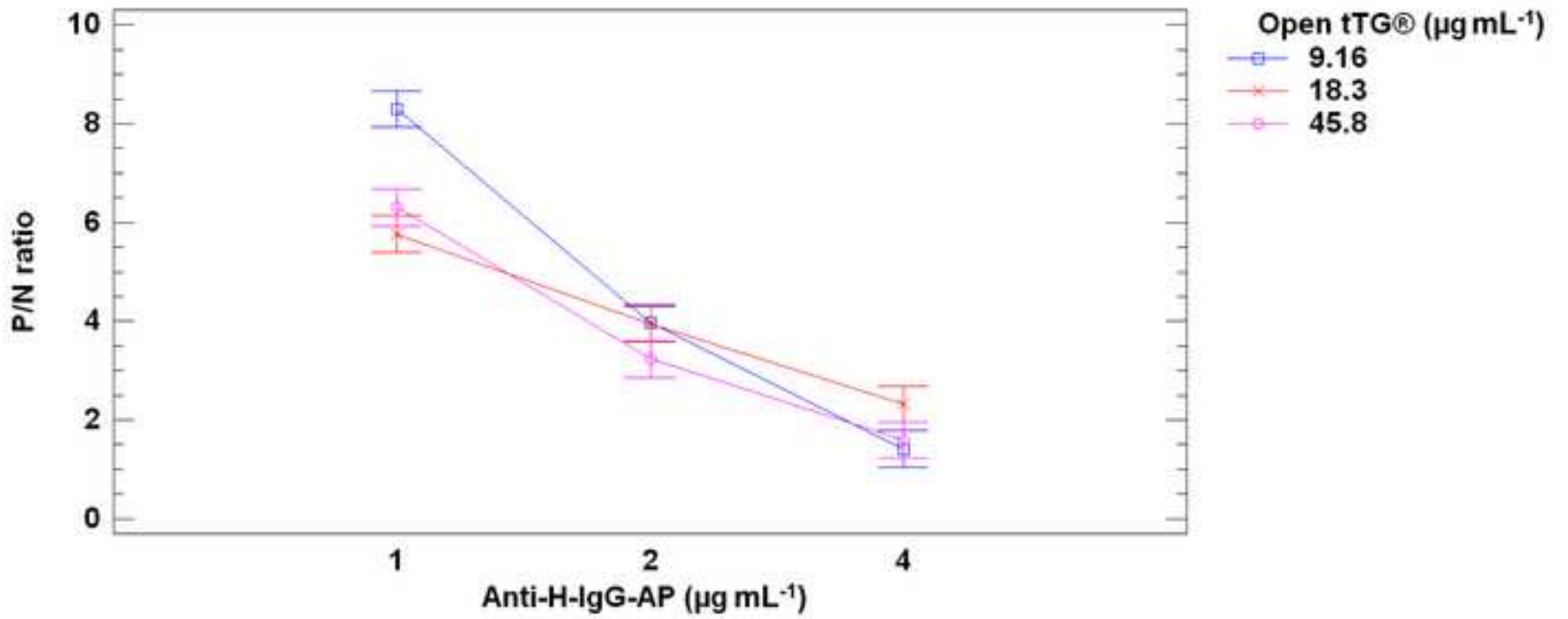


Figure 9
[Click here to download high resolution image](#)

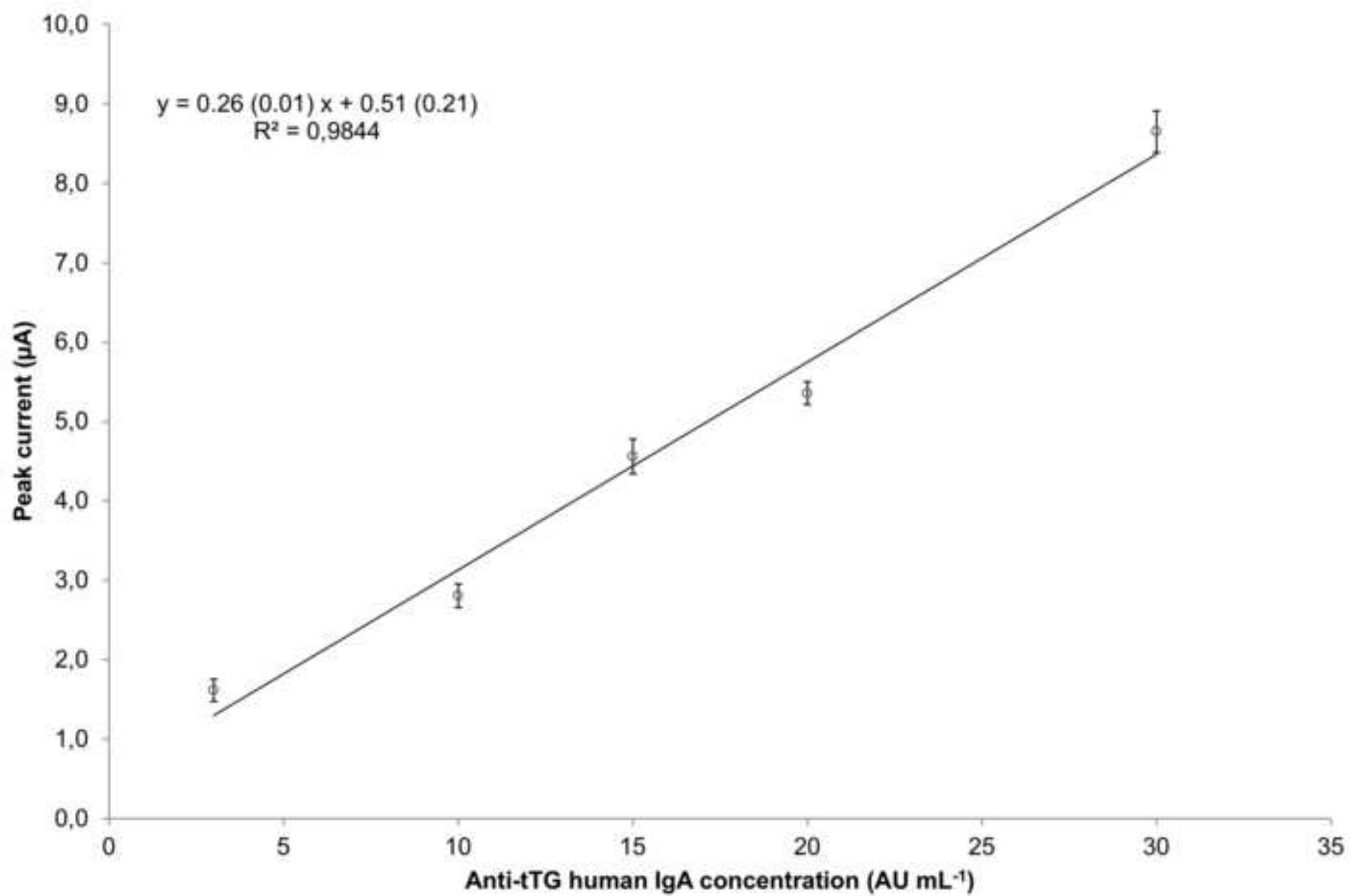


Figure 10
[Click here to download high resolution image](#)

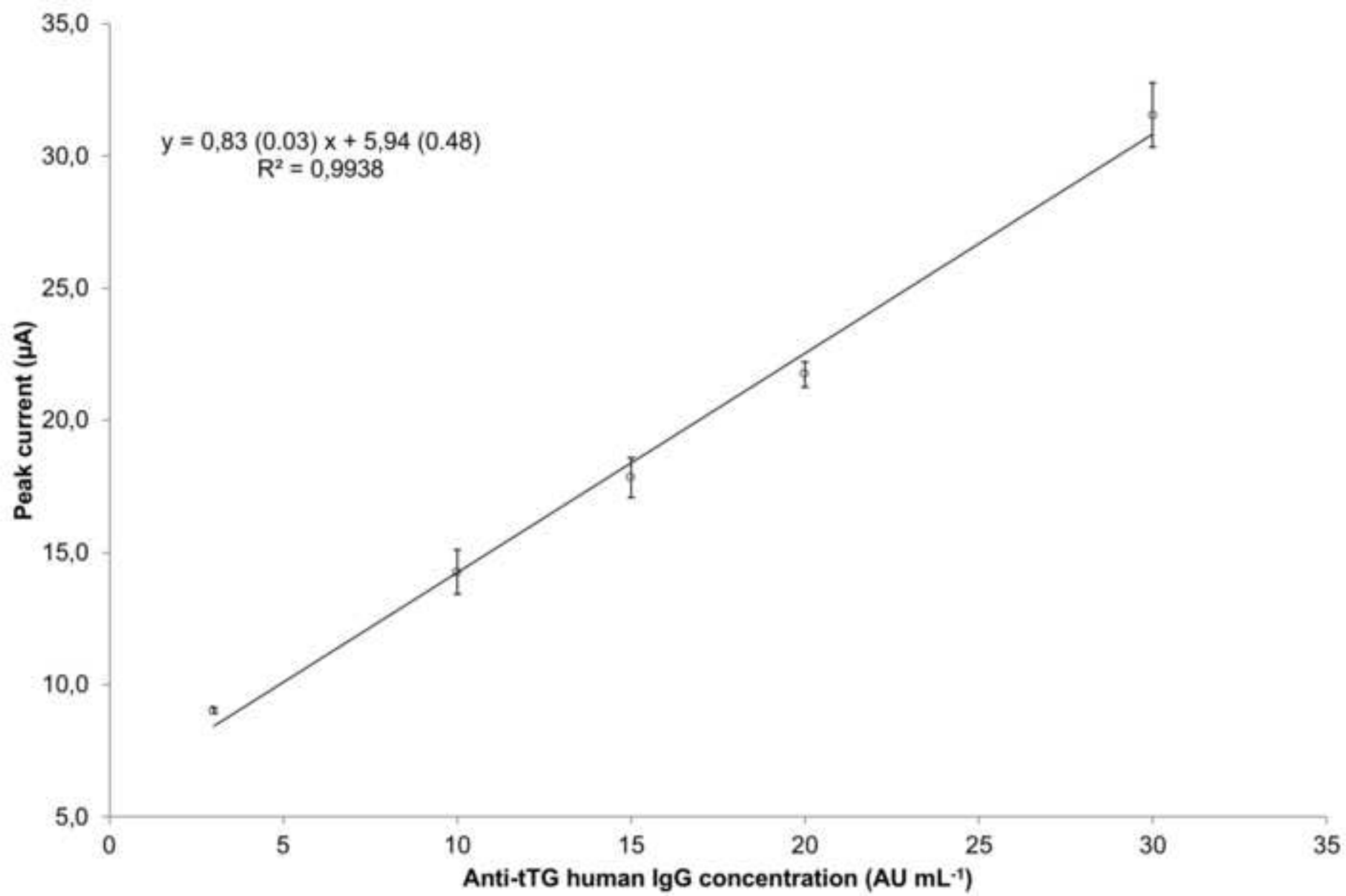


Figure 11
[Click here to download high resolution image](#)

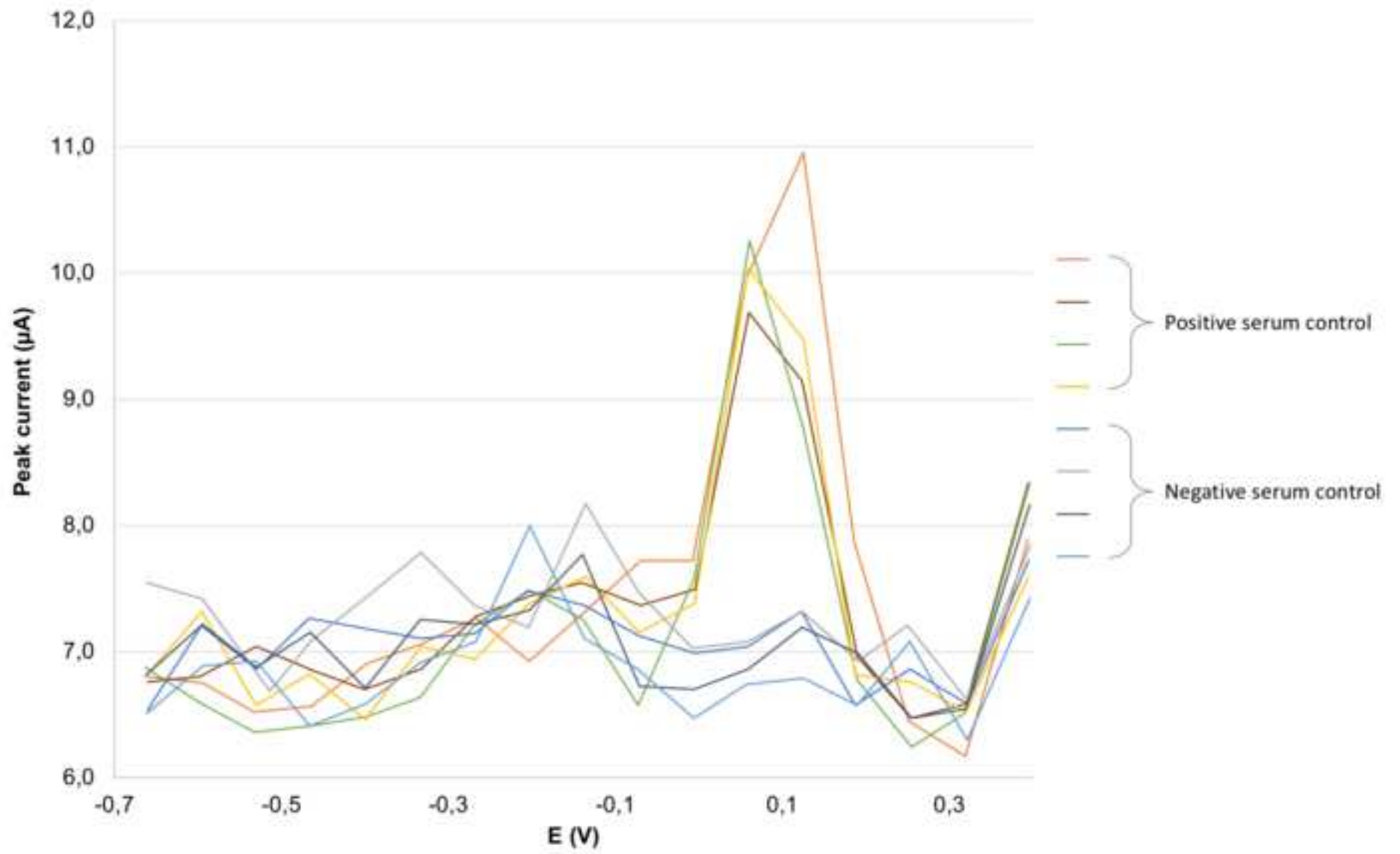


Figure 12
[Click here to download high resolution image](#)

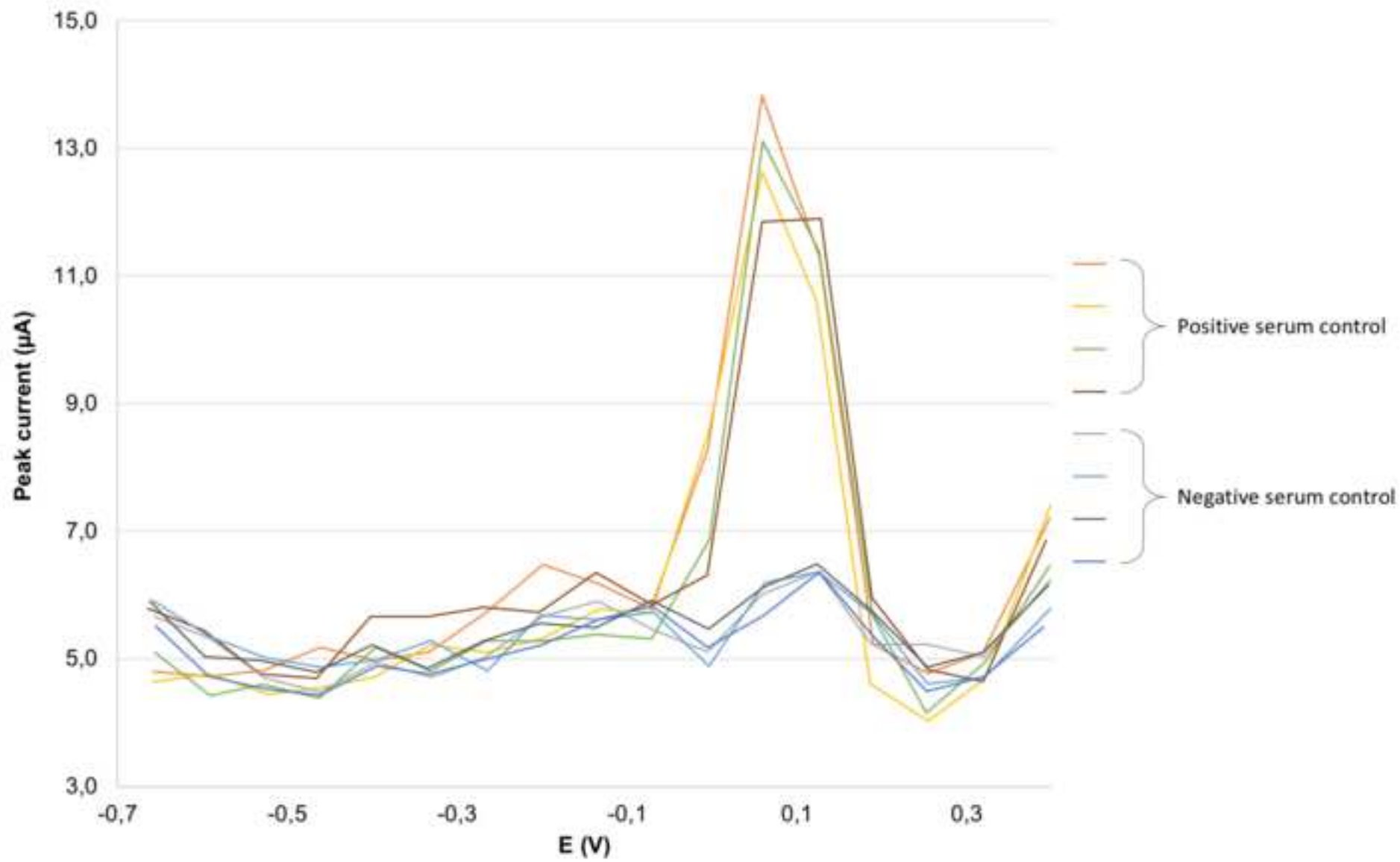


Figure 13

[Click here to download high resolution image](#)

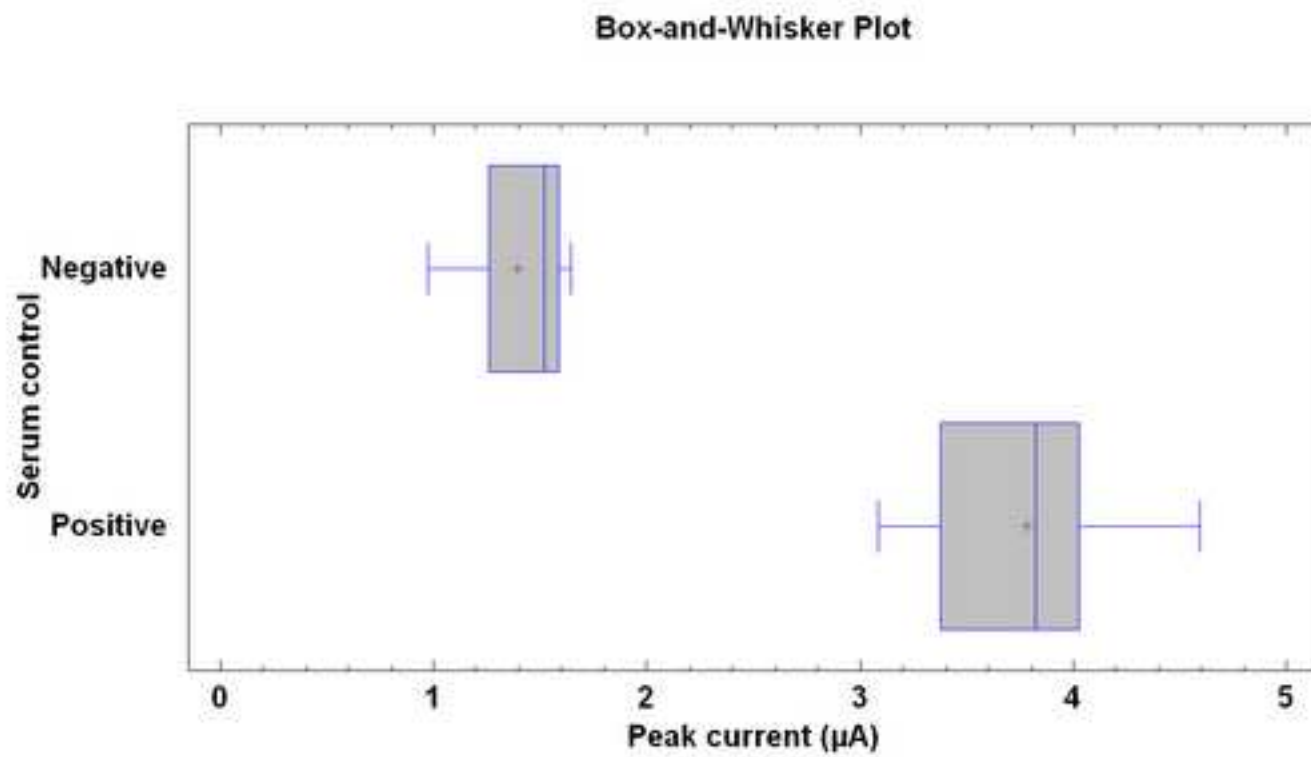
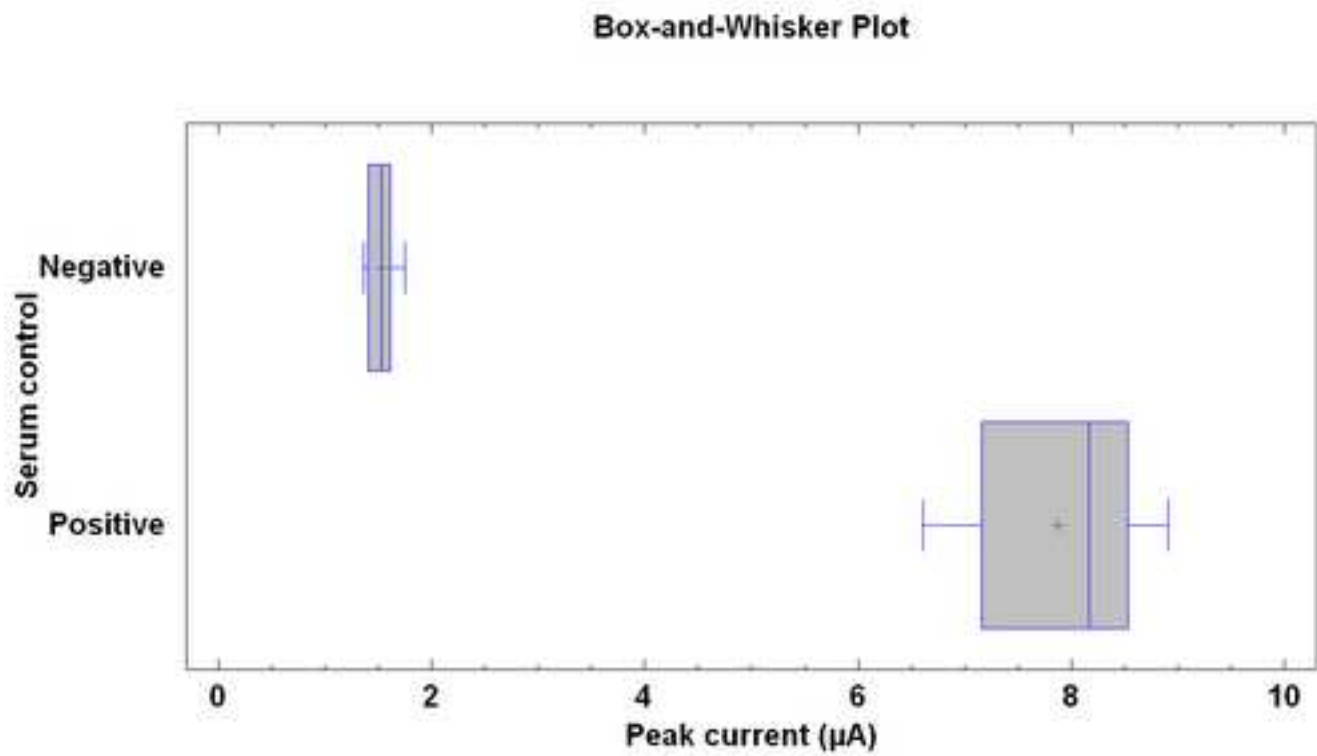


Figure 14
[Click here to download high resolution image](#)



Scheme 1. Schematic representation of the immunosensor set-up.

Figure 1. Developed prototype.

Figure 2. Architecture of the IoT Wi-Fi device (acquisition, processing and communicating sections).

Figure 3. Generated Bias voltage.

Figure 4. Generic architecture of a cloud-based system.

Figure 5. Currents measured in the cell with the related bias voltage applied.

Figure 6. Peak current and related baseline.

Figure 7. 2-way ANOVA interaction plot for Anti-tTG IgA antibodies.

Figure 8. 2-way ANOVA interaction plot for Anti-tTG IgG antibodies.

Figure 9. Immunosensor response to anti-tTG human IgA; inset: calibration function.

Figure 10. Immunosensor response to anti-tTG human IgG; inset: calibration function.

Figure 11. Signals recorded with the IoT-WiFi device for determination of anti-tTG human IgA.

Figure 12. Signals recorded with the IoT-WiFi device for determination of anti-tTG human IgG.

Figure 13. Box-and-whiskers plot for anti-tTG human IgA.

Figure 14. Box-and-whiskers plot for anti-tTG human IgG.

Biographies of authors

Marco Giannetto was born in 1973 and is Associate Professor of Analytical Chemistry at Parma University, Italy. He got his PhD in 2000 at Parma University. He teaches Analytical Chemistry and “Sensors and Screening Techniques” for the bachelor’s and master’s degrees in Chemistry. His current research interest is focused on the design, realization, characterization and validation of new chemical sensors and biosensors based on different transduction mechanisms with applications in clinical diagnosis and point-of-care, food safety/quality control and environmental monitoring.

Valentina Bianchi received the B.Sc. and M.Sc. (summa cum laude) degrees in electronic engineering and the Ph.D. degree from the University of Parma, Italy, in 2003, 2006, and 2010, respectively. Since 2006, she has been with the Department of Information Engineering, University of Parma. Since 2017, she has been with the Department of Engineering and Architecture, University of Parma, as Research Assistant. She participated in several national and international projects. She has authored or co-authored of more than 30 papers published on technical journals or proceedings of international conferences. Her current research interests include wireless sensors networks and digital systems design.

Silvia Gentili was born in 1990 and recently got her master’s degree in Chemistry at Parma University, Italy discussing a thesis dealing with the development of innovative immunosensors for diagnosis of celiac disease based on an IoT-Wi-Fi board. She is a Research Collaborator at Parma University and her current research interest is focused on the thermodynamics of metal complexes in solution.

Simone Fortunati was born in 1990 and is currently attending the PhD course in Chemical Sciences at the University of Parma, Italy. He graduated in Biomolecular Chemistry in 2016. The topic of his PhD work is focused on the employment of innovative nanomaterials and bioreceptors for the development of biosensors, such as genosensors aimed at the detection of transgenic material at trace levels, immunosensors for detection of anti-transglutaminase antibodies using an IoT-WiFi device for DPV signal acquisition and sensitive electropolymerized coatings for compounds of environmental concern.

Ilaria De Munari received the Electronic Engineering degree from Parma University (Italy) in 1991. She got the Ph.D. degree in Information Technologies in 1995. From 1997 she was with the Dept. of Information Engineering (the present Dept. of Engineering and Architecture) of Parma University, first as Research Assistant and from 2004 as Associate Professor of Electronic. Her research interests were initially focused on the reliability of semiconductor devices and on the design of low-power digital integrated circuits and power-aware applications, cooperating to several national and international projects. For some years, she participated in several activities related to assistive technologies, managing some projects in the framework of Ambient Assisted Living (AAL) Joint Programme in collaboration with other European partners. Currently, she is involved in research activities related to the design of electronic systems for Human Activity Recognition (HAR) and, in general, for healthcare problems based on microcontroller and FPGA solutions. She is author or co-author of more than 100 papers published on technical journals or proceedings of International conferences.

Maria Careri is Full Professor of Analytical Chemistry at Parma University, Italy, since 2001. Chair elected of the Executive Board of the Division of Analytical Chemistry of the Italian Chemical Society (2007 – 2009), she is Member of the Editorial Board of Current Analytical Chemistry and of Analytical and Bioanalytical Chemistry. Her research activities have centered on the development of novel materials for solvent-free extraction techniques, the development and validation of methods based on mass spectrometry techniques, and the development of innovative immunosensing devices for the determination of biomarkers in cancer screening programmes and for celiac disease as well as of compounds of environmental and food interest